



Comparison of motion sickness incidence of three crew transfer vessels with different hull forms

Héloïse Vignal

Master Thesis

presented in partial fulfillment

of the requirements for the double degree:

“Advanced Master in Naval Architecture” conferred by University of Liege
“Master of Sciences in Applied Mechanics, specialization in Hydrodynamics,
Energetics and Propulsion” conferred by Ecole Centrale de Nantes

developed at West Pomeranian University of Technology, Szczecin

in the framework of the

“EMSHIP”

Erasmus Mundus Master Course

in “Integrated Advanced Ship Design”

Ref. 159652-1-2009-1-BE-ERA MUNDUS-EMMC

Prof. Zbigniew Sekulski, West Pomeranian University of
Technology, Szczecin

Supervisor: Michael Luehder, Naval Architect, Abeking & Rasmussen,
Lemwerder, Germany

Reviewer: Prof. Florin Pacuraru, University of Galati (UGAL)

Szczecin, February 2014



Master Thesis developed at West Pomeranian University of Technology, Szczecin

CONTENTS

1. INTRODUCTION.....	11
2. HISTORICAL BACKGROUND OF SEAKEEPING ANALYSES AND TYPE OF SHIPS FOR COMPARATIVE STUDIES.....	13
2.1. Evolution of seakeeping researches.....	13
2.2. Small Waterplane Area Twin Hulls.....	14
2.3. Crew transfer vessels.....	16
2.4. Hull form advantages and drawbacks.....	17
2.4.1. Resistance.....	17
2.4.2. Stability.....	18
2.4.3. Propulsion.....	19
2.4.4. Capacity distribution.....	20
2.4.5. Seakeeping.....	20
2.4.6. Conclusion.....	20
3. PROBLEM.....	21
3.1. Motion sickness phenomenon.....	21
3.2. Limiting criteria.....	23
3.3. Motion Sickness Incidence (MSI).....	24
4. METHODOLOGY.....	26
4.1. Coordinate systems and encounter frequency.....	28
4.2. Linear seakeeping theory.....	29
4.2.1. Linear theory.....	30
4.2.2. Frequency domain approach.....	31
4.3. Method used for the exploitation of the experimental results.....	35
4.3.1. Numbering of the tests and description.....	35
4.3.2. Tests series.....	36
4.4. <i>Seakeeper</i> software to perform the numerical analysis.....	38
4.4.1. Hull definition and inputs.....	38
4.4.2. 2D-linear strip theory, software precisions.....	39
4.4.3. Postprocessor.....	40

4.4.4.	Software and strip-theory limitations	40
4.4.5.	Validation of the results	42
5.	MONOHULL ANALYSIS	44
5.1.	Preliminary design	44
5.1.1.	Design specificities	44
5.1.2.	Similar ships	44
5.1.3.	Hydrostatics.....	46
5.1.4.	Lines plan	48
5.1.5.	Structural weight	49
5.1.6.	General arrangement	53
5.1.7.	Vertical position of the centre of gravity	56
5.1.8.	Conclusion.....	56
5.2.	Numerical model used for the monohull analysis	57
5.2.1.	Hull measurement	57
5.2.2.	Inputs data	57
5.2.3.	Results and MSI-curves	59
6.	CATAMARAN ANALYSIS	67
6.1.	Preliminary design	67
6.1.1.	Similar ships	67
6.1.2.	Hydrostatics.....	68
6.1.3.	Lines plan	69
6.1.4.	Structural weight	70
6.1.5.	General arrangement	71
6.1.6.	Weight estimation of the catamaran.....	74
6.1.7.	Vertical position of the centre of gravity	74
6.2.	Numerical model for the catamaran analysis	75
6.3.	Results and MSI-curves for the catamaran.....	76
7.	CONCLUSIONS	82
8.	ACKNOWLEDGEMENTS	84
9.	REFERENCES.....	85

List of figures

Figure 1 : High speed craft concepts based on Keuning's researches (1994)	13
Figure 2 : <i>Natalia Bekker</i> , 25m-SWATH [www.maritimejournal.com, 02/12/2013]	14
Figure 3 : Comparison of water plane areas for same waterline length of a monohull, a catamaran and a SWATH [www.abeking.com, 06/2013].....	15
Figure 4: Main characteristics of SWATH with a single strut configuration [www.SWATH.com, 04/2013]	15
Figure 5 : Time to reach the wind-farms from Table 1 in function of the average speed of the boat.....	17
Figure 6 : Rolling angles response of a six foot wave [www.stabilityyachts.com, 01/06/13].	18
Figure 7 : Righting moment comparison between catamaran and monohull [www.boatdesign.net, 06/2013]	19
Figure 8 : Empirically derived relationship of MSI to frequency and acceleration over two hours [5]	22
Figure 9 : Severe discomfort boundaries - ISO 2631 - 0,1 to 0,63 Hz for z-axis vibrations [5]	24
Figure 10 : Cumulative distribution function of the random variable z [1].....	25
Figure 11 : Aspect of Motion Sickness Incidence curve for different vertical accelerations and same peak period [<i>Seakeeper Manual</i>].....	26
Figure 12 : Methods to compare the MSI of the three different hull forms.....	27
Figure 13 : Translation motions of ships.....	28
Figure 14 : Rotation motions of ships	28
Figure 15 : Ship encountering waves [<i>Seakeeper manual</i>].....	29
Figure 16 : Obtaining of the ship response spectrum graphically – Catamaran, 5 knots, 2m-135° waves	30
Figure 17 : Linear response of the ship – Response Amplitude Operator (RAO)	30
Figure 18 : Excitation force due to the wave [Seakeeping lectures, Pierre Ferrant – Ecole Centrale Nantes, 04/2013].....	34
Figure 19 : Position of the accelerometers [experimental report, A&B]	35
Figure 20 : Numbering of the physical tests	36
Figure 21 : Numbering of the monohull and catamaran numerical analyses.....	36
Figure 22 : Transversal hull sections mapped according to the Lewis’s conformal mapping procedure for a monohull [<i>Seakeeper manual</i>]	38

Figure 23 : Operationnal speeds definition [<i>Seakeeper software</i>]	39
Figure 24 : Choice of analysis methods	40
Figure 25 : Typical half breadth ratio mapped by the conformal Lewis's method.....	41
Figure 26 : Range of aspect ratio and area coefficient of Lewis forms [Theoretical manual Seaway – Delft University, report 1216a, February 2001]	42
Figure 27 : Design specificities of the monohull	44
Figure 28: Comparative monohulls.....	45
Figure 29 : Lines plan of the 33m monohull.....	48
Figure 30 : Spiral design of ship [www.marinewiki.org, 17/12/13]	49
Figure 31 : Preliminary structure of the monohull.....	51
Figure 32: General arrangement of the monohull (profile view).....	54
Figure 33: General arrangement of the monohull (deck views).....	55
Figure 34 : Roll and pitch gyradii of the monohull.....	57
Figure 35 : Position of the remote locations	58
Figure 36 : JONSWAP spectra for the 5 and 10 knots tests	61
Figure 37 : MSI-curves comparison between the monohull and the SWATH for 5 and 10 knots speed	62
Figure 38 : Monohull RAO and MSI-curves comparison with the <i>Duhnen</i>	65
Figure 39 : Lines plan of the 25m-catamaran	69
Figure 40 : Scheme for selection of rules to be applied according to the 4 main criteria [9] ..	70
Figure 41 : Profile view and bridge general arrangement of the catamaran	72
Figure 42 : General arrangement of main and below deck of the catamaran.....	73
Figure 43 : Vessel type definition according to Maxsurf model.....	75
Figure 44 : JONSWAP spectra used for the seakeeping analyses	76
Figure 45 : Results for the 5 and 10 knots simulation of the catamaran	78
Figure 46 : RAOs of the catamaran and her MSI-curves compared to the SWATH.....	79

List of tables

Table 1 : European wind farms and required time to reach the installations according to the speed [www.Wikipedia.com, 05/2013].....	16
Table 2 : Comparison of the different hull forms main characteristics.....	20
Table 3: Limiting criteria in term of vertical acceleration [5].....	23
Table 4 : Usual convention representing the different DOF of a ship	28

Table 5 : 2000 and 2003 full scale tests concerning the <i>Duhnen</i> – darker boxes represent the tests.....	36
Table 6 : Original significant wave heights of the experiments done the 27th January 2000 .	37
Table 7 : Peak frequencies of the experimental tests	37
Table 8: Typical values of the pitch and roll gyradius [source: <i>Seakeeper</i> manual].....	39
Table 9 : Typical table of <i>Seakeeper</i> results (Catamaran – 5 knots – Head seas)	43
Table 10 : Characteristics of the comparative ships.....	45
Table 11 : General geometric characteristics of the monohull.....	46
Table 12 : Hydrostatics of the monohull [<i>Hydromax</i> analysis]	47
Table 13 : Estimation of the structural weight according to Grubisic	50
Table 14 : Weight structure comparison between the SWATH and a similar monohull.....	50
Table 15 : Weight of the sets.....	52
Table 16 : Lightship weight estimation and centre of gravity.....	52
Table 17 : Tanks definition	52
Table 18 : Weight balance of the "Go offshore" load case	56
Table 19 : Weight balance of the "go home" load case.....	56
Table 20 : JONSWAP spectra definition from the <i>Duhnen</i> experiments	58
Table 21 : Results for the 5 and 10 knots simulation between the Monohull and SWATH (peak encounter frequencies)	59
Table 22 : Difference in term of percentage of seasick people on board after 10, 50 and 2 hours on board.....	63
Table 23 : Evolution of MSI curve through tendency curves	63
Table 24 : Tendency curve equations of the MSI-curves comparison between SWATH and Monohull at 8 and 12 knots.....	66
Table 25 : Comparative table of the results from the Bremen's Hochschule and the comparative monohull.....	66
Table 26 : Characteristics of the comparative catamaran	67
Table 27 : Main characteristics of the catamaran.....	68
Table 28 : Hydrostatics of the catamaran – full loaded load case condition.....	68
Table 29 : Estimation of the structural weight of the catamaran [6].....	70
Table 30 : Main elements of the lightship weight.....	74
Table 31 : Position of the centre of gravity of the tanks and the « go offshore » load case	75
Table 32 : Simulation conducted with the catamaran	76

Table 33 : Maximal significant vertical acceleration and peak frequencies of the catamaran analyses	77
Table 34 : Trend curves for the catamaran MSI and SWATH.....	80
Table 35 : Difference in term of motion sickness incidence between the Catamaran and the SWATH.....	80

Declaration of Authorship

I, Héloïse Vignal declare that this thesis and the work presented in it are my own and has been generated by me as the result of my own original research.

Where I have consulted the published work of others, this is always clearly attributed.

Where I have quoted from the work of others, the source is always given. With the exception of such quotations, this thesis is entirely my own work.

I have acknowledged all main sources of help.

Where the thesis is based on work done by myself jointly with others, I have made clear exactly what was done by others and what I have contributed myself.

This thesis contains no material that has been submitted previously, in whole or in part, for the award of any other academic degree or diploma.

I cede copyright of the thesis in favour of the University of

Date:

Signature

ABSTRACT

The Crew Transfer Vessels (CTV) which operate near offshore installations rarely sail in calm water. The rough sea conditions produce ship motion such as vertical accelerations that affect people on board. It may cause sea sickness. The increasing number of offshore wind farms in North Sea has increased the number of sea keeping studies to reduce the time transfer even when the weather is bad and avoiding sickness motion. High vertical acceleration peaks could induce voluntary speed reduction and loss of money. A Small Water-plane Area Twin Hull (SWATH), a monohull and a catamaran (CTV configuration) will be compared using motion analysis and the influence on humans. The purpose of this master thesis is to prove that the seakeeping behaviour of the SWATH is better than monohull and catamaran hull forms. My work started during my internship at Abeking & Rasmussen between July and September 2013.

There are different indexes to estimate the sea sickness phenomenon, depending mainly on the wave frequency, the vertical acceleration and the time of exposure. The oldest one is the Motion Index Incidence (MSI) to estimate quantitatively the impact of ship motions in the percentage of people that would suffer from seasickness. The ISO rules established the human body limits, function of the duration of exposure. By calculating the MSI index, it is possible to estimate the percentage of sick people in different localization on the deck according to the wave spectrum, ship speed and heading angle.

The SWATH is known for its good sea keeping behaviour due to its small water plane area. Physical tests have been done in North Sea in 2000 and 2003; the vertical accelerations and time-domain wave elevations were measured in different localizations on the 25m-SWATH *Duhsen*. The experimental significant wave amplitude and wave spectrum (frequency domain) were calculated to define the wave spectrum for the two numerical sea-keeping analyses of the monohull and the catamaran. The analyses presented in the thesis are realized with the *Seakeeper* software, a plug-in of the *Maxsurf-naval architectural suite*. The 2D-stip theory is used by *Seakeeper* to calculate the hydrodynamic coefficients.

The preliminary design of the comparative hull forms are based on existing designs, recent studies and berthing to the offshore installations. The 33m-monohull has the same displacement than the SWATH and the catamaran the same length. The numerical results will be compared together with the MSI values obtained from the experimental measurements of the *Duhsen*.

Nomenclature

BV	Bureau Veritas
CG	Centre of Gravity
CTV	Crew Transfer Vessel
DOF	Degree Of Freedom
ESC	Enlarged Ship Concept
GL	Germanischer Lloyd classification society
GRT	Gross Tonnage
IMO	International Maritime Organisation
JONSWAP	Joint North Sea Wave Project
MSI	Motion Sickness Incidence
OPV	Offshore Patrol Vessel
RMS	Root Mean Square
SQM	Square Meter
SVA	Significant Vertical Acceleration
SWATH	Small Waterplane Area Twin Hull
TCB	Transversal Centre of Buoyancy

1. INTRODUCTION

During the last decades, a particular attention has been given to ships' seakeeping characteristics. It comes from the increasing of offshore installations close to the coast but also the fact that customers take in consideration the comfort of the passengers together with the optimization of time transfer to the wind farms. With the improvement of computational tools, it is now possible to include seakeeping calculation during preliminary design stage. The 2D-strip theory is widely used because it is low time consuming.

One way to improve the comfort on board is reducing the seasickness risk by analysing motion sickness indexes. Motion sickness is a phenomenon known by anyone using cars, bus, trains, ferries or airplanes. It can be described by the mismatch theory which stipulates that when the brain receives different information from the inner ear and the visual system, it reacts and produces discomfort until vomiting.

The motion sickness incidence (MSI) predicts the percentage of crew and passengers which will be sick after some time on board. It is function of the wave frequency, the significant wave height, the RMS vertical acceleration and the time of exposure. This principle has been introduced by McCaughey [1]. It is based on a study conducted with 300 young male students exposed to vertical accelerations at different frequencies inside a simulator.

The number of patrol boats and CTV is increasing since a few decades. They are seaworthy even at high speed in rough sea conditions. New seakeeping friendly concepts appeared such as the enlarged ship concept (ESC) and the axe bow concept. Both are hull form evolution from conventional monohull form. The axe bow concept is the continuity of the first concept established by Keuning in collaboration with the University of Delft in Nederland [2]. The two comparative designs are based on these evolutions and on the accessibility to the offshore installations.

Experiments have been ever conducted with SWATH vessels, such as with the *Duhnen* in January 2000 in north Deutschland by the shipyard Abeking & Rasmussen, near to Cuxhaven and in 2003 by the Bremen's university to measure her response motions. The purpose was the measurement of vertical accelerations in five different locations on the bridge. Many results from different speed and heading angles were available to compare with the numerical analyses of this master thesis. There were accessible during my internship in summer 2013. The final purpose of this master thesis is to prove that less people are sick on SWATH than on catamaran or monohull concepts.

The comparative numerical simulations were done with the software *Seakeeper*® which is a module of the *Maxsurf-suite*. The nurbs-lines modeller *Maxsurf* has been used to design the hull forms, *Hydromax* to determine the position of the tanks and do the preliminary weight estimation. The vertical centre of gravity position is an input data to run the seakeeping analysis. *Workshop* was used in this thesis to create the 3D-structure of the ships.

The preliminary design of the monohull was composed of a hull shape, a simplified superstructure, a static stability analysis and preliminary weight estimation. Some data were available online along with the knowledge of the company which design also monohull yachts. The simplified structural design was done according to the Bureau Veritas classification rules.

The preliminary catamaran design was a more complex task due to the lack of data. The axe-bow concept is protected by a patent which belongs to the University of Delft and the DAMEN's shipyard. The design is a hull like an axe-bow catamaran based on existed ships. The structure was designed according to the Germanischer Lloyds rules to perform the weight estimation of the multi-hull to finally deduce the vertical position of the centre of gravity.

2. HISTORICAL BACKGROUND OF SEAKEEPING ANALYSES AND TYPE OF SHIPS FOR COMPARATIVE STUDIES

2.1. Evolution of seakeeping researches

The crew transfer vessels can be classified as high speed vessels according to the IMO definition [3], equation (10). Up to the end of the 1960s, the research and design optimization for high speed vessel were mainly focused on water resistance and stability (Stavitsky 1968) in spite of the seakeeping aspect. The understanding of seakeeping characteristics of planning hulls and high speed vessels started with noteworthy work of Van den Bosch (1970), Fridsma (1969-1971) and Martin (1978) among others.

The standards defining the limitation in term of vertical accelerations and passenger comfort appeared at the end of the XXth century. They boosted seakeeping research field. The influence of the fore shape close to the bow on response motion and accelerations in waves was noticed by Blok and Roeloffs in 1989.

A lot of new advanced concepts for high speed craft emerged during the last decades of the XXth century, Figure 1. These new concepts were generally optimized in term of wave resistance by minimizing the displaced volume or wetted surface. A series of motion control devices were added to minimise the motion response but these solutions were really expensive.

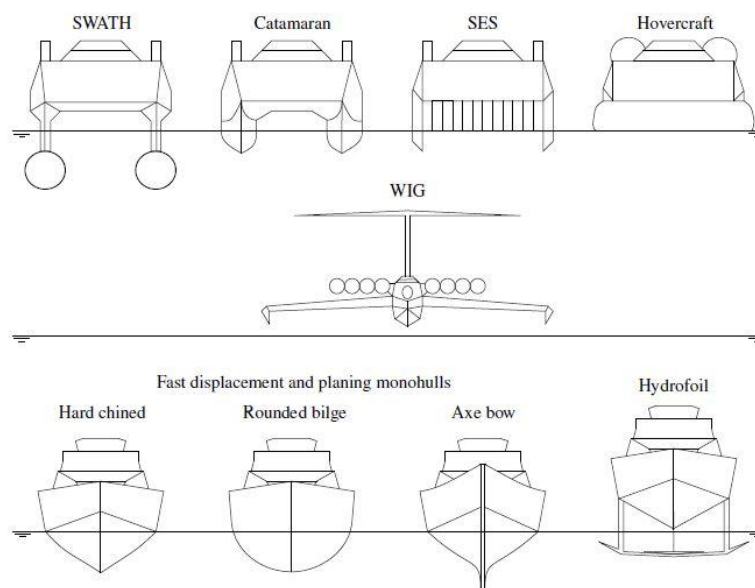


Figure 1 : High speed craft concepts based on Keuning's researches (1994)

The apparition in 1970s of the catamaran led to a boost in the field of high-speed ferries. The Small Waterplane Area Twin Hull (SWATH) is a derivative of the catamaran. The first idea of this advanced design came from a British Royal Navy captain, Captain Beadon who proposed in 1860 such a basic configuration.

At the end of the XXth century, the high speed vessels are more and more used for costal and even open sea operation for patrol and offshore duties. This new market generated new concepts for seaworthy high speed monohull such as the Enlarged Ship Concept (1995) and the Axe Bow Concept (2001).

2.2. Small Waterplane Area Twin Hulls

The Small Waterplane Area Twin Hull (SWATH, Figure 2) is a twin-hull ship design that minimizes hull volume in the surface area of the sea, also called water plane area.



Figure 2 : *Natalia Bekker*, 25m-SWATH [www.maritimejournal.com, 02/12/2013]

By minimizing hull volume in the sea's surface, where wave energy is located, the vessel becomes more stable, even in rough seas and at high speeds. A comparison of waterplane area for three different hull forms is presented Figure 3.

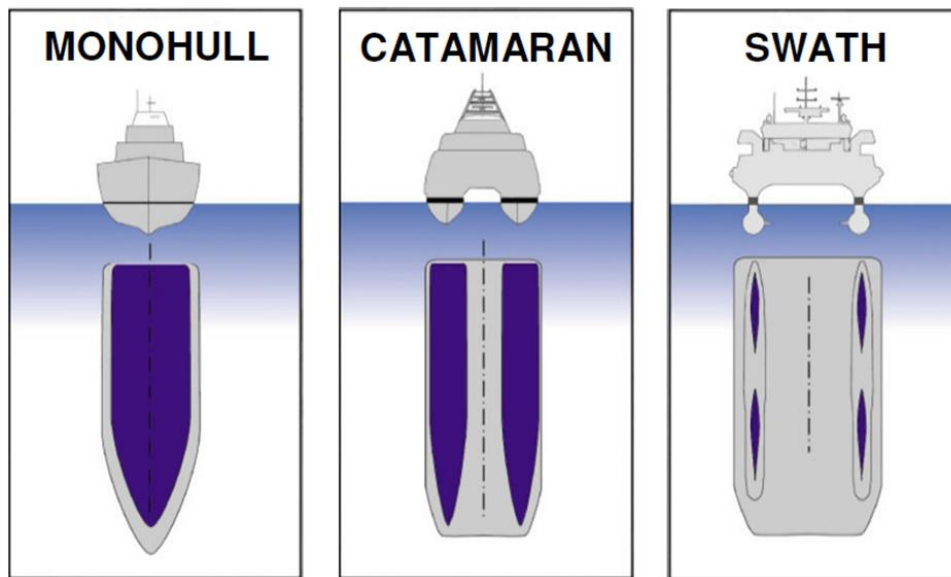


Figure 3 : Comparison of water plane areas for same waterline length of a monohull, a catamaran and a SWATH [www.abeking.com, 06/2013]

The buoyancy of the SWATH is provided by its submerged bodies, which are connected to the upper platform by single or twin struts, Figure 4. The bulk of the displacement necessary to keep the ship afloat is located beneath the waves, where it is less affected by wave action. The wave excitation drops exponentially with depth. Placing the majority of the ship's displacement under the waves is similar in concept to submarines and offshore rigs, which are also not or less affected by wave action.

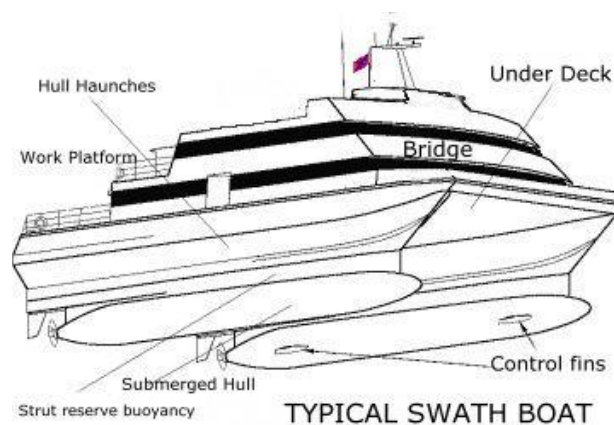


Figure 4: Main characteristics of SWATH with a single strut configuration
[www.SWATH.com, 04/2013]

The SWATH form was invented by Canadian Frederick G. Creed, who presented his idea in 1938 and was later awarded a British patent for it in 1946. It was first used in the 1960s and

1970s as an evolution of catamaran design and used for oceanographic research vessels or submarine rescue ships.

The shipyard Abeking & Rasmussen, located in Lemwerder in Germany is a twin hull specialist. They produced their first SWATH during the 1970ies and are now able to design and deliver SWATH ships reliable for tough everyday duty.

2.3. Crew transfer vessels

CTV are designed to mainly transport offshore support personnel, to and from their working places on different offshore installations. In addition it may also be used to transport the personnel's equipment and other bigger cargo. The boat might also be able to conduct rescue operations. The study is focused on small crew transfer vessels operating on the European wind farms installations, Table 1. They are accessible in less than two hours for a vessel with a average speed of 10-12 knots, Figure 5. The percentage of sick people will be estimated for a maximum of two hours trip.

Table 1 : European wind farms and required time to reach the installations according to the speed
[www.Wikipedia.com, 05/2013]

	Wind farm	Capacity (MW)	Year	Number of turbines	km to shore	Nationality
1	Blyth Offshore	4	2000	2	1.6	UK
2	Scroby sands	60	2004	30	2.5	UK
3	Lynn and Inner Dowsing	194	2009	54	5	UK
4	Gunflet Sand 1&2	172	2010	48	7	UK
5	Kentish Flats	90	2005	30	10	UK
6	Hywind	2.3	2009	1	10	Norway
7	Thanet	300	2010	100	11	UK
8	OWEZ	108	2008	36	13	Netherlands
9	Sheringham Shoal	317	2012	88	17	UK
10	Hrons Rev I	160	2002	80	18	Denmark
11	Greater Gabbard	504	2012	140	23	UK
12	Beatrice	10	2007	2	23	UK
13	Princess Amalia	120	2008	60	26	Netherlands
14	Thorntonbank	30	2009	6	27	Belgium
15	Horns Rev II	209	2009	91	32	Denmark
16	Alpha Ventus	60	2010	2x6	56	Germany

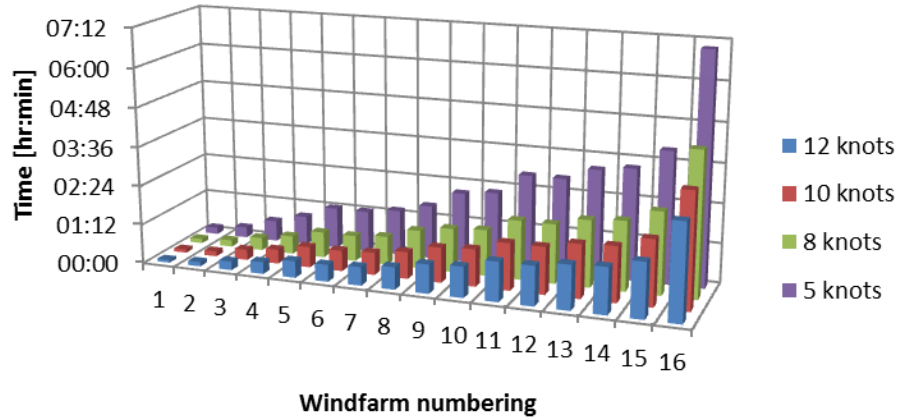


Figure 5 : Time to reach the wind-farms from Table 1 in function of the average speed of the boat

2.4. Hull form advantages and drawbacks

Choosing a hull form depends on many parameters those will be compare in the next subparts. The monohull, catamaran and SWATH configurations are used for crew transfer vessels.

2.4.1. Resistance

- For a monohull, the lower resistance is reached for the minimum displacement and a high length by beam ratio.

“A monohull with L/B ratio of fifteen will still have a higher resistance than a catamaran with a L/B ratio equal to six” [7].

- The resistance of a catamaran is mainly governed by the spacing between the two demihulls. The moment of inertia of the ship is equal to the sum of the one for each demi-hull multiply by the waterline surface and the square of the half distance between the hulls. For a slender hull such as the demi-hulls of a catamaran, the width is small compared to the length, the underwater volume is small but the resistance due to the total width of a catamaran is high.

- The resistance of SWATH in calm water is affected by her large immersed volume. The lower hulls induce frictional resistance; the space between them is bigger than for a catamaran with a similar displacement. The frictional drag is reduced with larger underwater hull space. The large spacing has a negative effect on the resistance. The slenderness of the hull is limited by the lower hulls and the wave making resistance is bigger. The maximum wave making resistance is reached for a Froude number equal to 0.5. To counteract these additional resistances, the length of the SWATH is often smaller than for a conventional ship. The weight of the immersed parts is reduced. So, a small water plane area makes necessary wider hull spacing.

2.4.2. Stability



Figure 6 : Rolling angles response of a six foot wave [www.stabilityyachts.com, 01/06/13]

- For a monohull, the intact stability is directly related to the weight. The value of the upright moment is limited by the ship's form. It depends on the magnitude of weight shifted to the centre of buoyancy in the transversal plane. The maximum value for the shifting to the buoyancy centre is $\frac{1}{4}$ of the beam. A narrow and deep hull has a high metacentric height, then a better transversal stability but short rolling period resulting in high acceleration at the deck level, Figure 6.
- Usually, intact stability puts no constraints when designing multi-hulls ships. The transversal stability is much better for multi-hull ships. When a catamaran starts to roll, one of the hulls goes outside of the water and the other one inside the water, which cause the TCB to shift a lot. The righting lever; lever arm between CB and CG is large. It means that the recovery moment to straighten the ship is high, Figure 7.

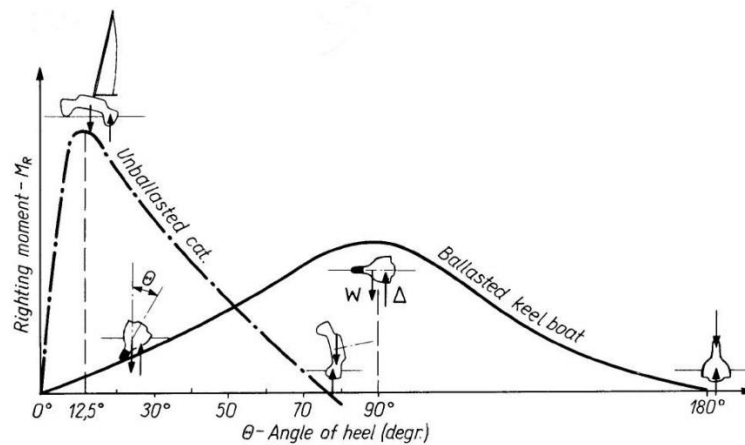


Figure 7 : Righting moment comparison between catamaran and monohull [www.boatdesign.net, 06/2013]

The evolution of the GZ-curve for small heeling angle of a similar SWATH is similar to the GZ-curve of a monohull. For higher heeling angle, the SWATH should have a GZ-curve close to the catamaran but SWATH never reaches heeling angle higher than 20° due to her important immersed volumes.

The longitudinal metacentric height of a SWATH is lower than a similar catamaran (lower centre of gravity) then the roll and pitch natural periods are longer. The moment of inertia along the longitudinal axis is greater for SWATH that is why her natural rolling period is globally twice high than for a comparable monohull. The natural heaving period is also longer. The longitudinal metacentric height is two or three times smaller than a comparable monohull, while the moment of inertia along the transversal axis is the same. Consequently, the natural pitching period of SWATH is usually twice higher.

2.4.3. Propulsion

Monohulls are generally equipped with one water jet instead of two, so there is a gain in term of machinery weight in despite of manoeuvrability which is less efficient with one rudder instead of two.

The resistance of a SWATH ship is higher than the one of a catamaran. For an equivalent amount of power, the speed will be lower for the SWATH. Moreover the installation is more complex due to the struts slenderness.

2.4.4. Capacity distribution

The capacity distribution of a monohull is limited by her transverse stability, i.e her length by beam ratio. The catamaran capacity is often one and a half to two times bigger than for a similar monohull. 40-50% of the total capacity is generally inside the hulls and the rest goes on the cross-structure. For a SWATH, the capacity distribution is distributed as follow: 15-20% in the struts, 20-25% in the submerge volumes and 55-65% in the cross-structure in the case who it is as long as the hulls. The SWATH is considered as a platform without payload in inner spaces. The small waterplane area characteristic induces a high sensibility to load charges.

2.4.5. Seakeeping

Short rolling period for catamaran can cause great discomfort of passengers and crew members, oven appearance of motion sickness, which can be the main obstacle for choosing marine transportation. With her lower centre of gravity, the SWATH has longer natural rolling period.

The purpose of this work is to prove that the SWATH has a better seakeeping behaviour in rough seas than the two other hull forms. The seakeeping behaviour of the ships are studied in this thesis.

2.4.6. Conclusion

The results of the comparative work are presented in the Table 2.

Table 2 : Comparison of the different hull forms main characteristics

	SWATH	Catamaran	Monohull
Resistance	-	++	+
Transverse stability	++	+	-
Propulsion	-	+	++
Capacity distribution	+	++	-
Seakeeping	++	+	-
Cost	-	+	++
Structure complexity	-	+	++

‘++’ is given for a criteria which gives an advantage to a specific hull form, ‘-’ for a drawback in comparison to the two others hull forms and ‘+’ neither. Each hull form has advantages and drawbacks in term of main arrangement and hydrodynamic properties and the ship hull form selection should be very detailed discussed.

3. PROBLEM

The main goal of this study is the comparison of seasickness between a monohull similar in term of displacement to the SWATH and a catamaran similar in term of length to the SWATH-*Duhsen*. There are three crew transfer vessels for European offshore installations.

The seasickness phenomenon is represented in term of motion sickness incidence index (MSI). The Motion Sickness incidence index expresses the percentage of person on-board which will vomit after a certain time of exposure.

The seakeeping characteristics of crew transfer vessel are really important because without good ship motion responses, the crew will reduce the speed, the time transfer will be increase and finally it could induce a loss of profit. These studies take in consideration the significant behaviour of the ship into a specific seaway by taking in consideration the significant wave heights and significant vertical accelerations.

The monohull is 33m long and the catamaran 25m with a lower displacement than the SWATH. The comparison is done with high seakeeping capabilities ships. A preliminary study concerning the hull shape has been conducted to obtain seakeeping friendly similar hulls. Preliminary designs include hull definition, weight repartition and stability.

The monohull and catamaran responses to a similar sea state are expressed in term of significant vertical accelerations (SVA) which are used to draw the MSI-curves. The SWATH MSI-curves have been drawn from the experimental SVA.

3.1. Motion sickness phenomenon

Motion sickness or kynetosis is the sickness associated to motion. It is a term to describe the discomfort and associated breathing irregularities, warmth, disorientation and vomiting. The motion sickness comes from mismatching information received by the brain. The vestibular apparatus in the inner ear provides the brain with information about self-motion that does not match the perception of motion received by the visual system. Receiving contradictory information from two different organs, the tendons and muscles near the stomach joint and induce vomiting.

Many factors can induce motion sickness. There can be physiological, environmental and emotional factors. People suffering of agoraphobia or old persons are predisposed to seasickness.

The vertical acceleration is one of the main factors at the origin of motion sickness. It is expressed as significant or root mean square accelerations. The significant vertical acceleration, $a_{1/3}$, represents the highest one-third of the vertical accelerations measured during a certain period of time. The root mean square magnitude of vertical acceleration is the half of the significant acceleration, see equations (1) and (2).

$$a_{1/3} = 2 * a_{RMS} \quad (1)$$

$$a_{RMS} = \sqrt{(a_m - a_1)^2 + (a_m - a_2)^2 + \dots + (a_m - a_n)^2} \quad (2)$$

With a_m , the average accelerations and a_i which have been measured during the experiments at constant time steps.

The other parameter responsible of motion sickness is the ship response frequency for a given significant wave height and wave frequency.

The mathematical expression of the motion sickness incidence has been established by McCaughley [5] and al which is depicted in Figure 8. The percentage of sick people depends on the ship frequency and RMS vertical acceleration.

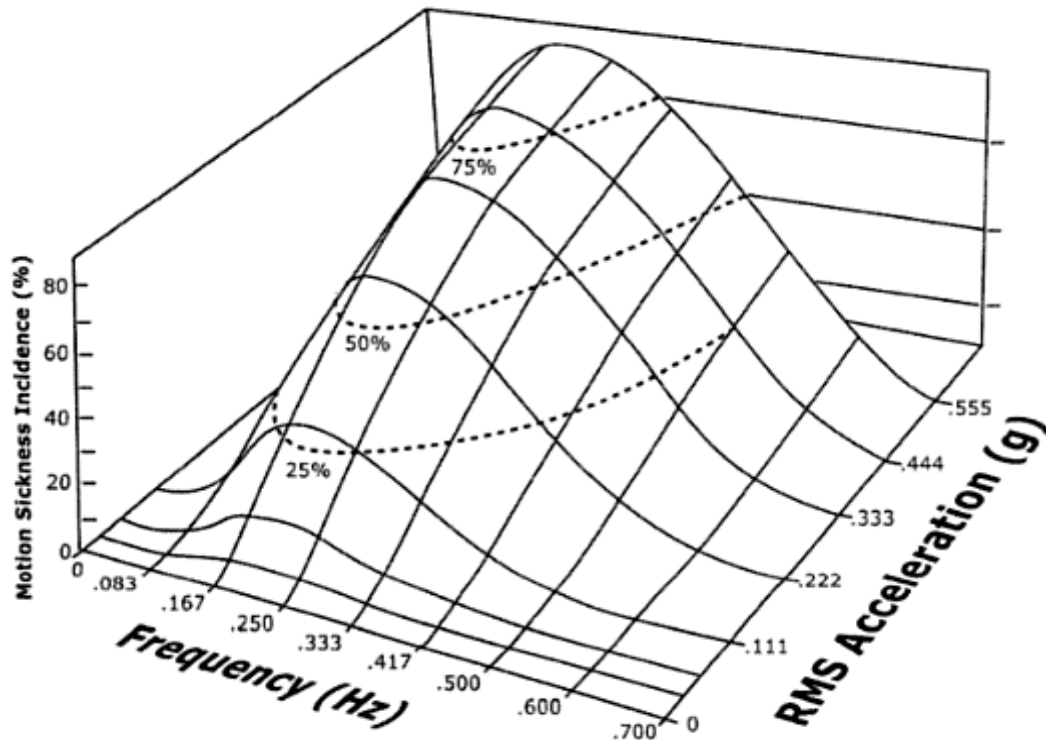


Figure 8 : Empirically derived relationship of MSI to frequency and acceleration over two hours [5]

At higher and lower frequencies the stimulus is progressively less provocative. The incidence of sickness increases as a function of the intensity of the oscillation, but even a stimulus

having RMS amplitude of less than 1 m/s^2 is provocative at 0.2 Hz. The worst ship frequency is around 0.167Hz.

3.2. Limiting criteria

The International Standard ISO 2631-1 “Mechanical vibration and shock – Evaluation of human exposure to whole-body vibration” (ISO Standard 2631-1, 1997) defines methods of quantifying whole-body vibration in relation to human health and comfort, the probability of vibration perception and the incidence of motion sickness.

The International Standard ISO 2631 is composed of 3 parts:

- Part 1 – General requirements,
- Part 2 – Continuous and shock-induced vibration in buildings (1 to 80 Hz),
- Part 3 – Evaluation of exposure to whole-body z-axis vertical vibration in the frequency range 0,1 to 0,63 Hz.

The third part concerns the motion sickness which is defined for a frequency below 1 Hz; ship motion response is not considered as a vibration phenomenon. The thresholds of RMS vertical acceleration are defined in the Table 3.

Table 3: Limiting criteria in term of vertical acceleration [5]

Limiting criteria for vertical acceleration (RMS)	
0.02 g	Passengers on a big cruise liner
0.05 g	Passengers on a ferry
0.10 g	Normal work for the crew
0.15 g	Heavy work for adapted crew
0.20 g	Ligth work for adapted crew
0.275 g	Simple works

Many indexes have been developed to estimates the impact of ship motion on the human body, the seasickness phenomenon or the incapability to work properly.

Seakeeping performance index is a term used to assess the motion and dynamic effects for a given sea state, direction of heading angle and speed of transit. Generally these indices, such as MSI, are good for short trips because over longer periods, a few hours or a few days, adaptation of the motion occurs and the sensibility of humans to motion sickness decay too.

For a wide range of frequencies, the MSI curve of the ship response can be plot over the motion sickness discomfort boundaries to express the discomfort on-board, Figure 9.

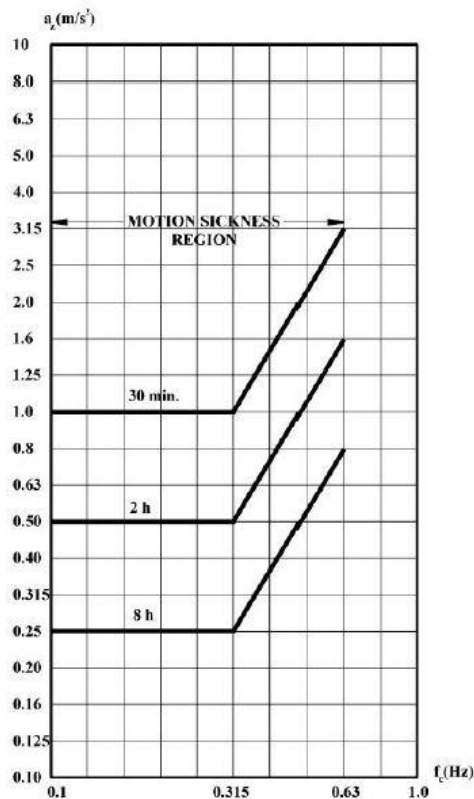


Figure 9 : Severe discomfort boundaries - ISO 2631 - 0,1 to 0,63 Hz for z-axis vibrations [5]

The sea is a superposition of linear waves at different frequencies and wave height. The Figure 9 shows that if the vertical acceleration is equal to 1,0g and the ship response frequency between 0.1Hz and 0.315Hz then people will be sick in 30 minutes. By considering only the significant peak period the worst case is highlighted instead of the all range of frequencies.

3.3. Motion Sickness Incidence (MSI)

The MSI is an algorithm to predict the incidence of motion sickness induced by exposure of sinusoidal vertical accelerations. It has been established by a survey with young American male students exposed during two hours to sinusoidal vertical motions into a simulator. The conclusion of this experiment was that sickness is a cumulative effect related to vertical accelerations at certain frequencies (O'Hanlon and McCaughey from the office of naval research – 1970).

The Motion Sickness Incidence or percentage of subjects who vomit within two hours is mathematically expressed by the equation:

$$MSI(\%) = 100 * \theta(z_a) * \theta(z'_t) \quad (3)$$

with:

$$z_a = 2.218 * \log_{10}(a_z) - 9.277 * \log_{10}(f_p) - 5.809 * \log_{10}(f_p)^2 - 1.851 \quad (4)$$

$$z'_t = 1.134 * z_a + 1.989 * \log_{10}(t) - 2.904 \quad (5)$$

with a_z the SVA [m/s^2]

f_p the peak frequency of the ship response [Hz]

t the time of exposure [min]

$\Theta(z)$ the cumulative distribution function of the standardized normal random variable z , Figure 10.

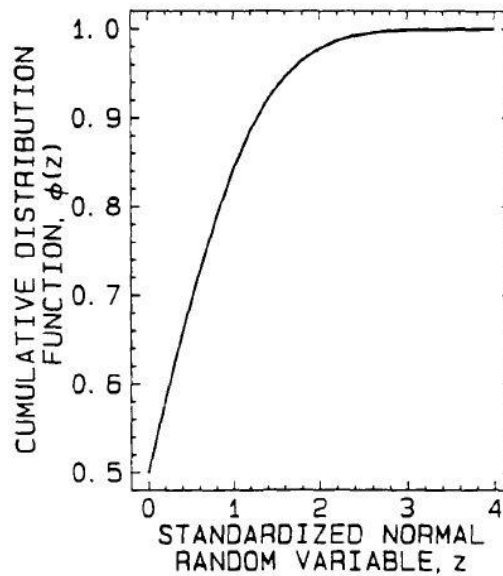


Figure 10 : Cumulative distribution function of the random variable z [1]

By using this function, the error between the experimental and mathematical results is 6%.

To obtain the MSI curves, the peak frequency of the ship response and the SVA have to be known. They will be deduced from physical results and numerical analyses.

4. METHODOLOGY

The comparison of seasickness on board has been done by comparing the MSI-curves of the three hull forms. The MSI curves representing the percentage of sick people on board have the same tend than the Figure 11 by taking the maximum SVA on the bridge of the ships.

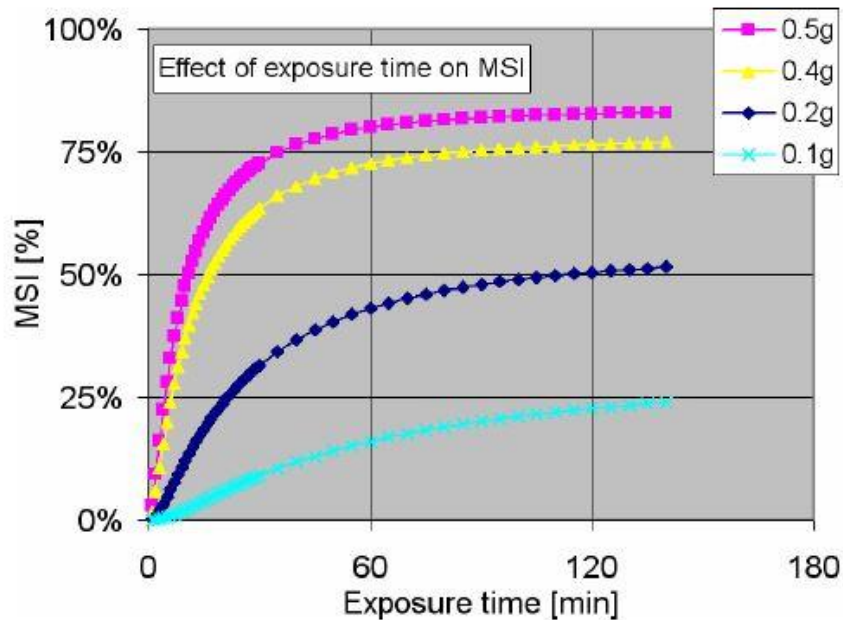


Figure 11 : Aspect of Motion Sickness Incidence curve for different vertical accelerations and same peak period [*Seakeeper Manual*]

The work layout is presented in Figure 12.

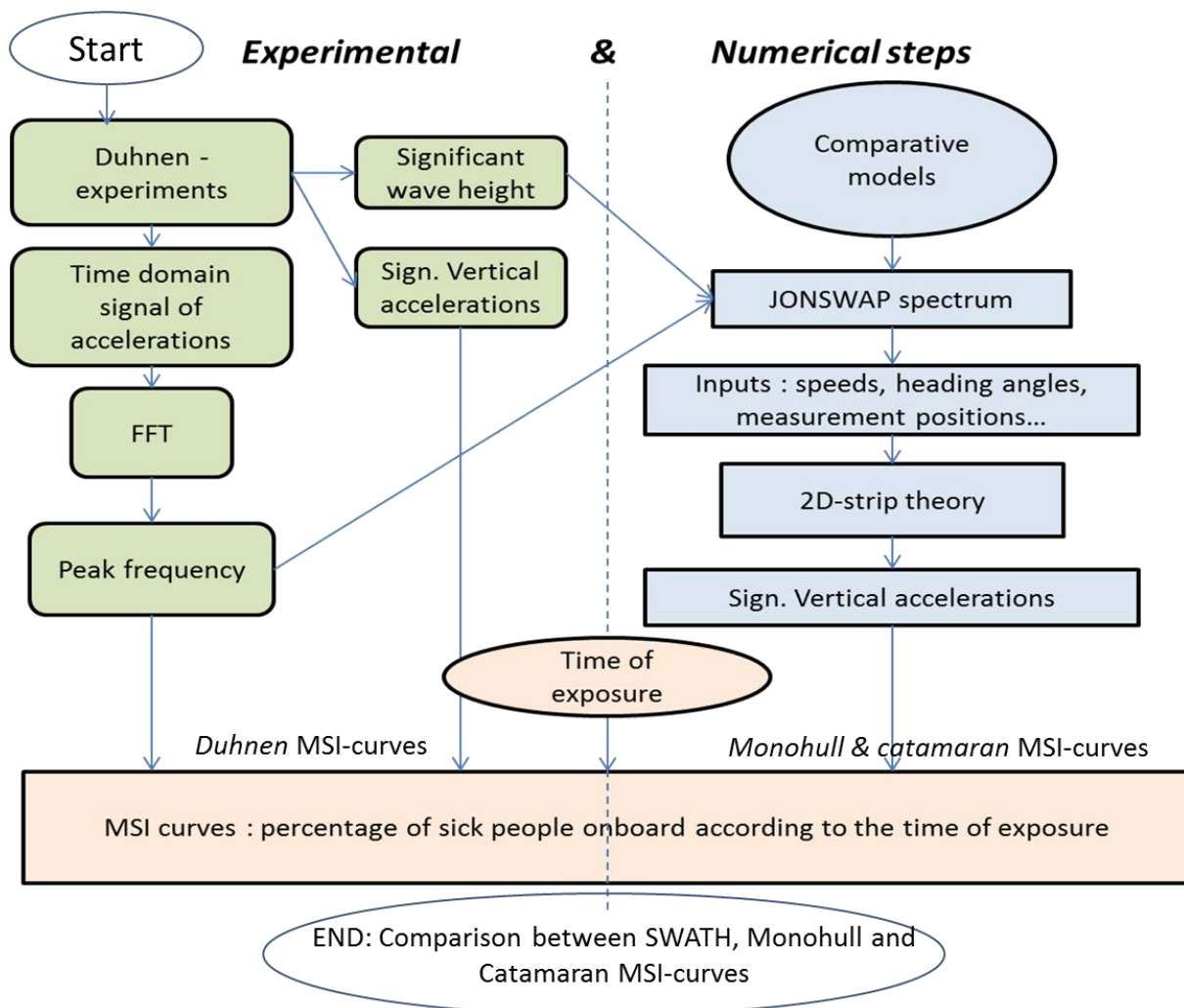


Figure 12 : Methods to compare the MSI of the three different hull forms

Initially the results from the *Duhnen* experiments have been analysed to determine the wave spectrum of the experiments and calculate the MSI-curves of the SWATH from the SVAs. The significant wave height and the peak frequency of the wave spectrum were used to define the JONSWAP wave spectrum which was entered as input of the numerical analyses. The speeds and heading angles are similar for the three ships. The right column represents the second part of the seakeeping analysis; the numerical models. The 2D-strip theory is used by *Seakeeper* to compute the vertical position at different locations on the vessel's bridges.

4.1. Coordinate systems and encounter frequency

The response of the ship is different for the six-degrees of freedom: heave, sway, surge in translation Figure 13 and roll, yaw and pitch in rotations Figure 14. During this works, three motions have been analysed: heave, pitch and roll.

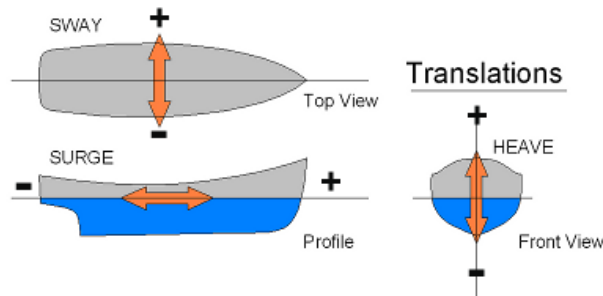


Figure 13 : Translation motions of ships

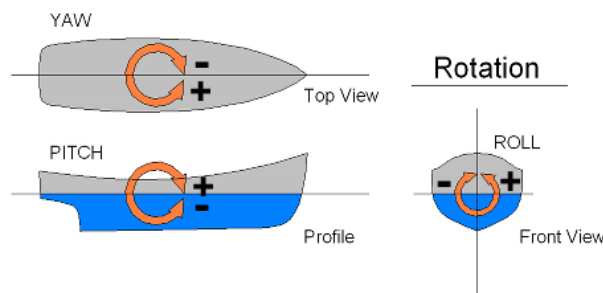


Figure 14 : Rotation motions of ships

The notation for the six DOF follows the usual convention:

Table 4 : Usual convention representing the different DOF of a ship

1	Surge
2	Sway
3	Heave
4	Roll
5	Pitch
6	Yaw

A ship encounters the waves with a different frequency in comparison to an external observer; this frequency is called the encounter frequency, Figure 15. It depends on the velocity of the waves c ; the velocity of the vessel U and the heading angle of the waves μ .

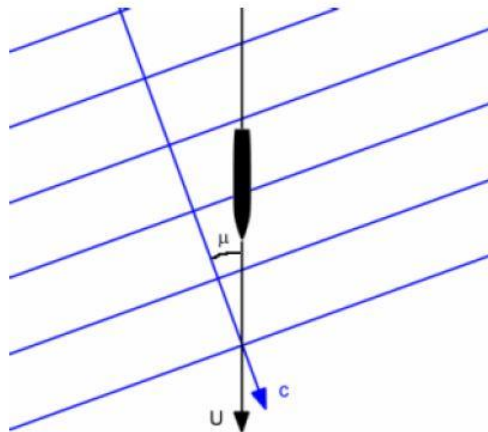


Figure 15 : Ship encountering waves [*Seakeeper manual*]

The mathematical definition of the encounter frequency is shown in the equation (6) and (7).

$$w_e = \frac{2\pi}{\lambda} * (c - U * \cos(\mu)) \quad (6)$$

According to the deep water assumption (see 4.2), the wave encounter frequency becomes

$$w_e = w - \frac{w^2 * U}{g} * \cos(\mu) \quad (7)$$

λ is the wave length [m], c the wave celerity [m/sec], U the ship speed [m/sec], μ the heading angle [rad] and k the wave number [1/m].

The encounter spectrum is a transformation of the wave spectrum from the vessel point of view which is travelling through the ocean at a certain speed. The peak frequency of the wave and encounter spectrum are linked by the relation (7).

4.2. Linear seakeeping theory

Until some decades ago, the seakeeping behaviour of ship was considered at the end of the spiral design of crafts (see 5.1.5, Figure 30) because of the expensive cost of model tests. New methods are now available to forecast the seakeeping behaviour of a ship without using ship models. They are less expensive, less time consuming and don't need physical installations (wave basins). Ship response in terms of response amplitude operators (RAO) is now accessible by computational analysis in a matter of minutes. The evaluation of seakeeping performances is heavily related to the wave environment and the criteria which are used to compare the designs. Many interrelating factors influence the seakeeping behaviour of a ship that is why it is difficult to predict their behaviours without dedicated software.

Different theories have been developed to compute seakeeping analyses. The simplest one is the linear 2D-potential flow method, called strip theory which consists of decompose the hull in transversal sections to compute the hydrodynamic forces. This method has been used for this thesis. More complex 3D-theories based on panel-method are becoming now widely used to compute ship motion responses.

The response of a ship to a specific sea state is represented by a transfer function such as electronic filters, Figure 17. The ship received an input, the sea state, filters it and produces a response which is the ship motion. The transfer function is called RAO. The ship response spectrum in heave S_z can be obtained graphically, Figure 16 by squaring the RAO spectrum of associated motion and multiplying by the wave encounter spectrum, equation (8).

$$S_z(w_e) = RAO^2(w_e) * S_w(w_e) \tag{8}$$

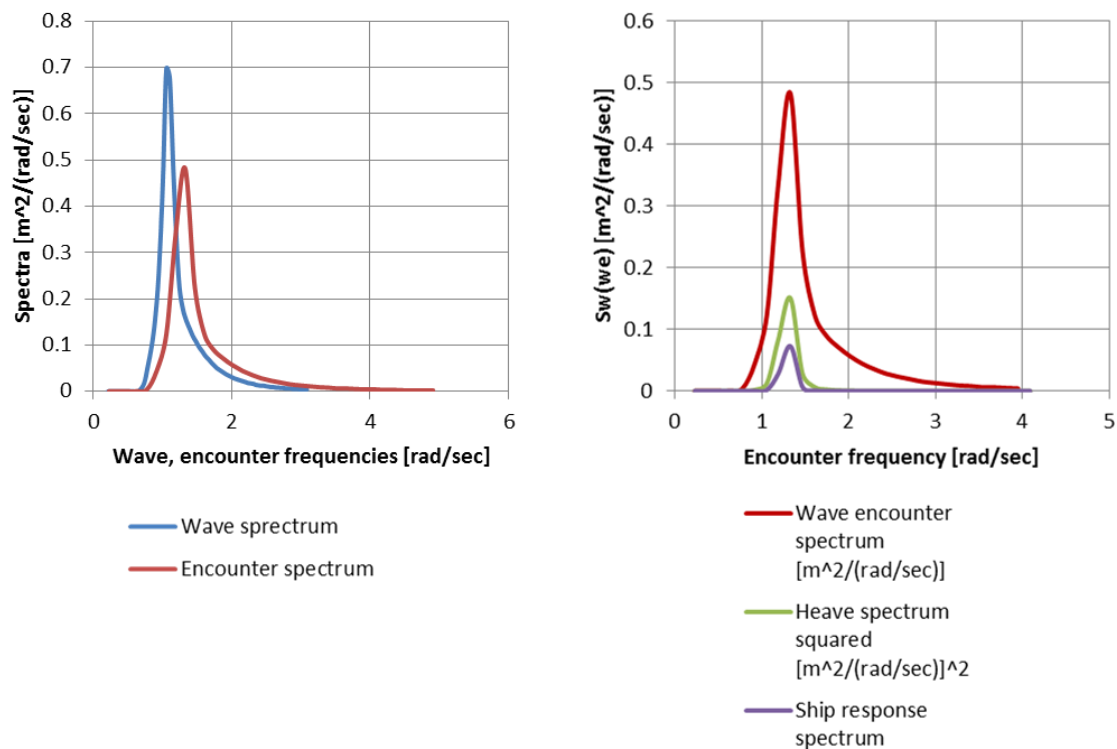


Figure 16 : Obtaining of the ship response spectrum graphically – Catamaran, 5 knots, 2m-135° waves

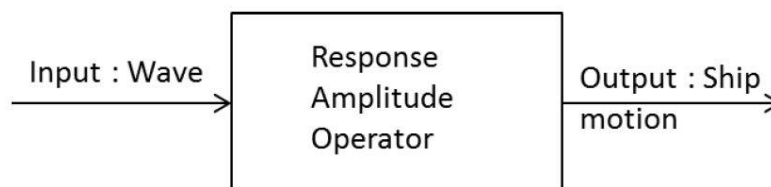


Figure 17 : Linear response of the ship – Response Amplitude Operator (RAO)

4.2.1. Linear theory

The linear theory in infinite water is based on the wave linearization which consists on decomposed the sea state in a combination of linear sinusoidal waves. The linear theory leads to first order results. The surface elevation of a linear wave in one dimension can be written:

$$\eta(x, t) = A * \cos(\omega t + kx) \quad (9)$$

with

- A the wave amplitude which is two time smaller than the wave height, noted h
- ω the wave pulsation [rad/sec] and
- k the wave number [rad/m], $k = 2\pi/\lambda$ with λ the wave length [m]

The linearity assumption is satisfied for limited wave steepness ε , to avoid breaking waves. The limiting steepness is given by the equation (10),

$$\varepsilon_{max} = \frac{H_{max}}{\lambda} = \frac{1}{7} \quad (10)$$

with ε_{max} the maximum wave steepness, H_{max} the maximum wave height and λ the wave length.

The infinite water depth assumption means that the linear wave is entirely described by its frequency ω and its amplitude in deep water, equation (11) is called the dispersion relation.

$$\omega^2 = g * k \quad (11)$$

With g the constant of gravitation.

Moreover the wave length λ can be deduced from the wave period T:

$$\lambda \approx 1.56 * T^2 \quad (12)$$

4.2.2. Frequency domain approach

The strip-theory used the frequency domain approach which consists of converting the time domain wave series in frequency domain. A wave spectrum resulting from this conversion is more easily analysable to assess the seakeeping analysis than time series data. The wave spectrum represents the energy distribution over frequencies. The ocean can be represented by many regular wave trains with different amplitude and phases. The wave field is represented by energy distribution over frequencies called wave spectrum.

The following assumptions are made when applying the strip theory [*Seakeeper manual*]:

- The vessel's motion are linear and harmonic

- The fluid is non-viscous, the viscous damping is ignored
- The ship is slender, i.e the length is much greater than the beam and the beam much less than the wave length
- The hull is rigid, no flexure when the wave length is much less than the ship length
- The speed is moderate and there is no dynamic lift
- The motion are linear with the wave amplitude, there are small
- The deep water wave may be applied
- The presence of the hull has no effect on the waves (Froude-Krylov hypothesis)

Under the linear theory approach, it is really convenient to write any variable x depending on time, in the following manner:

$$x(t) = \text{Re}(X_0 * \exp(-i\omega t)) = \text{Re}(X(t)) \quad (13)$$

with X_0 the complex amplitude independent of time and the phase.

The interesting variable X in seakeeping theory is one of the six DOF of the ship motion. The time derivatives are easily determined under this notation.

$$\dot{X}(t) = -i\omega X(t) \quad (14)$$

$$\ddot{X}(t) = -\omega^2 X(t) \quad (15)$$

The equation of motion of the boat is a vector of 6 components:

$$M\ddot{X} = F_{hydrostatic} + F_{Hydrodynamic} \quad (16)$$

M the mass matrix of the boat [6x6] multiplied by the acceleration is equal to the sum of the hydrostatic and hydrodynamics forces. The matrix is diagonal and its coefficients are equal to the displacement.

The [6x6] hydrostatic matrix is supposed to be known and is equal to the difference between buoyancy and gravity force. For small displacements, the hydrostatic matrix is simply the stiffness matrix,

$$F_{hydrostatic} = -[K_H]X \quad (17)$$

K_H the hydrostatic stiffness matrix.

The damping force, the wave excitation forces and the added mass are the three sources of the hydrodynamic force. The viscous effects are neglected, and then the damping force is proportional to the ship velocity. The added mass is proportional to the ship acceleration and the wave excitation is a radiation/diffraction phenomenon.

$$F_{Added\ mass} = [\mu] * w^2 * X \quad (18)$$

$$F_D = [\lambda] * \dot{X} = -iw * [\lambda] * X \quad (19)$$

$$F_{waves} = F_{incident} + F_{diffracted} \quad (20)$$

With

- $[\mu]$ the added mass matrix
- $[\lambda]$ the damping matrix

The equation of motion (15) becomes,

$$[-([M] + [\mu(w)]) * w^2 - iw[\lambda(w)] + [K_H]] * X = F_{incident}(w) + F_{diffracted}(w) \quad (21)$$

The vector of ship motion X is not the only one unknown of the problem. The stiffness and mass matrix are known from hydrostatic calculations and the incident wave depends on the body geometry and incident wave. Unfortunately, the added mass matrix, the damping matrix and the diffracted wave force have to be calculated before solving the equation (20).

Under the strip theory, the elements on the left part of the equation (20) are computed for each transverse strip of the ship and then there are integrated along the full length of the ship. The global added mass and the damping matrix are calculated according to the Salvesen et al. theory (1970) with two different formulations; the first one without transom stern and the second for ships with transom stern.

To compute the wave excitation force, equation (19), the problem is subdivided into two sub-problems, the radiation and diffraction problem. The radiation problem studies how the movement of the ship is affected by flat water and the diffraction one considers a fixed body in an incident wave field. The excitation force is depicted in the Figure 18 with the Froude-Krylov Force with is the radiated force and the diffraction force.

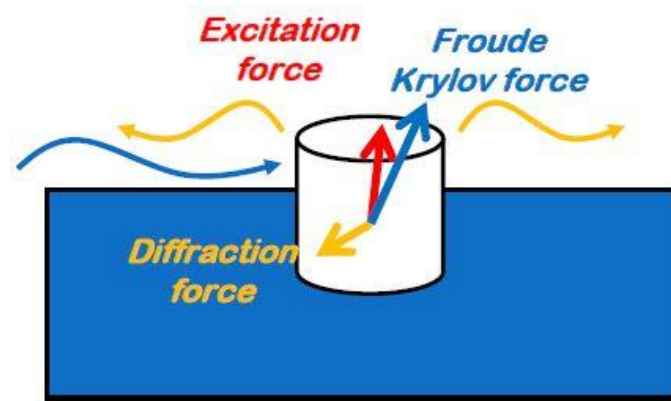


Figure 18 : Excitation force due to the wave [Seakeeping lectures, Pierre Ferrant – Ecole Centrale Nantes, 04/2013]

The Froude-Krylov force comes from the incident wave field which generates an unsteady pressure field and a force over the hull. The ship moves with a certain speed into the waves, a radiated wave field is generated and an associated unsteady pressure field. The radiated force is obtained by integration of the radiated pressure field over the hull shape.

The wave excitation force is obtained by two different ways. The simplest and quickest way is to assume that the waves are head seas waves, thus the Froude-Krylov and diffracted forces are simplified. Otherwise the computational time is longer and the equations to calculate the sectional excitation forces are more complicated.

4.3. Method used for the exploitation of the experimental results

Experimental results have been used to determine the percentage of sick people on board. The significant relative vertical accelerations were known from tables and the peak response frequencies have been obtained graphically with the response spectrum.

For each experiment done in 2000, the wave surface elevation was measured with a wave buoy and the vertical accelerations were registered in five locations on the bridge of the *Duhnen*, Figure 19. For the 2003 experiments, only four remote locations were used, two in the fore part and two in the aft of the bridge.

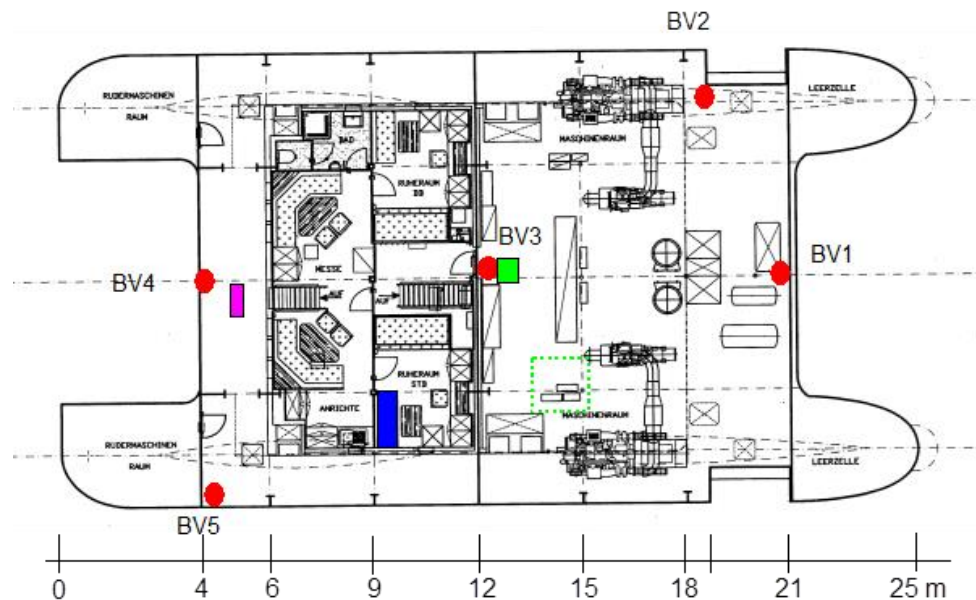


Figure 19 : Position of the accelerometers [experimental report, A&B]

4.3.1. Numbering of the tests and description

The SWATH experiments took place the 27 of January 2000 in North Sea. The numbering of the first series of experiments is related to the date and starts with 27. Then the two next numbers represents the forward speed of the ship and the three last numbers are the heading angle. The tests which have been conducted by student team in Bremen start with “HB”, which means Hochschule Bremen, then there are three □ for the speeds because there are two different tests at 12 knots and the last three “-“ represent the heading angle which is equal to 180° for all the tests, Figure 20.

27□ □ - - -
 HB□□□ - - -

Figure 20 : Numbering of the physical tests

Concerning the numerical analyses, the numbering is similar excepted for the first terms which start with a “M” for the monohull numerical analyses and a “C” for the catamaran, Figure 21.

M □□ - - -
 C □□ - - -

Figure 21 : Numbering of the monohull and catamaran numerical analyses

4.3.2. Tests series

The oldest results, from 2000, concern two speeds and five different heading angles, Table 5. Two more speeds, 8 and 12 knots, with different wave heights in head seas from the Hochschule Bremen were also studied.

Table 5 : 2000 and 2003 full scale tests concerning the *Duhnen* – darker boxes represent the tests

Speeds	Sign. Wave height [m]	Heading angles				
		Following seas	Beam seas	Quartering Bow	Head seas	Quartering stern
		0°	90°	135°	180°	315° (or 45°)
5	2					
8	2.4					
10	2					
12	1.5					
	2.4					
	Tests done					

By assuming that the ship response was linear with respect to the wave amplitude and the principle of superposition holds, the results from 2000 were calculated for the same significant wave height, 2 meters. The results are then comparable. In total 62 SVA were analysed and compared to the numerical results.

The original significant wave heights are exposed in the Table 6. The all tests at 5 and 10 knots were conducted the 27th January 2000 in North Sea near Cuxhaven, one round the morning and the other the afternoon.

Table 6 : Original significant wave heights of the experiments done the 27th January 2000

Series n°	Heading angle [°]	Significant wave height [m]
2710180	180	2.05
2710135	135	2.07
2710090	90	1.98
2710315	45	2.20
2710000	0	1.93
2705180	180	1.78
2705135	135	1.89
2705090	90	1.69
2705315	45	2.00
2705000	0	1.79

For the 2003 results, the response peak frequencies were deduced from the temporal acceleration signals by applying a fast Fourier transform. The signals were converted from time to frequency domain to get the peak frequency of the ship response, Table 7.

Table 7 : Peak frequencies of the experimental tests

Test n°	Peak frequency [Hz]
2705000	0.125
2705090	0.168
2705135	0.192
2705180	0.18
2705315	0.151
2710000	0.196
2710090	0.196
2710135	0.204
2710180	0.201
2710315	0.151
HB008180	0.127
HB012180	0.207
HB112180	0.127

With the peak frequency and the significant acceleration at one position, the MSI-curve has been drawn according to the McCaughley's mathematical representation. The curves look like the Figure 11 which represents the MSI-curves of a ship for the same encounter waves with different vertical accelerations.

4.4. *Seakeeper* software to perform the numerical analysis

Seakeeper is a module of the *Maxsurf*-suite dedicated to the ship motion analyses. It is composed of a pre-processor, a solver and a post-processor part. The computation is done by applying the 2D-strip theory.

4.4.1. *Hull definition and inputs*

The pre-processor steps consist on opening a design and defining the inputs data to run the numerical simulation.

The hull is at first created or imported on *Maxsurf*, the frame of reference and the draft are specified and save before opening it in *Seakeeper*. The vessel is longitudinally “cut” in a series of two-dimensional sectional strips. The hydrodynamic forces are evaluated independently on each 2D-section before being integrated along the total vessel length. The strip sections are defined by conformal mapping, using the Lewis procedure. Regularly spaced transverse sections are calculated along the waterline, Figure 22.

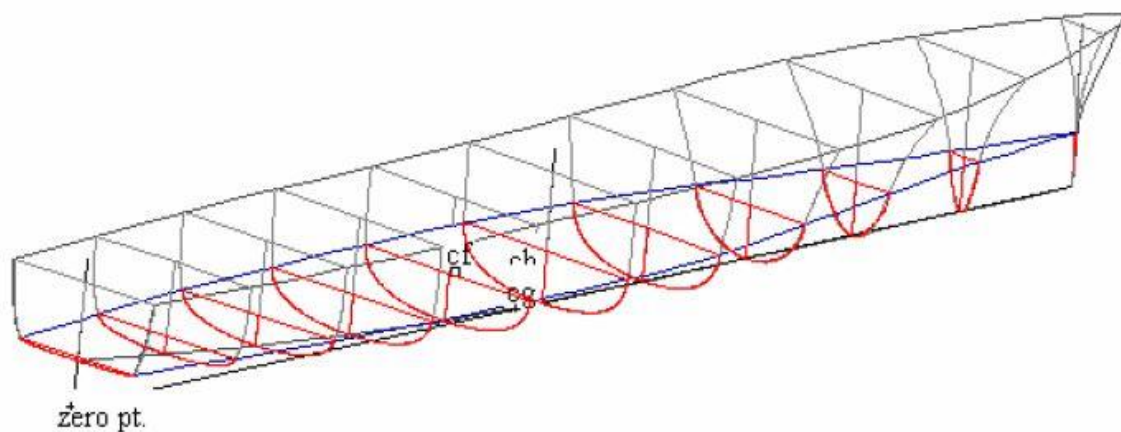


Figure 22 : Transversal hull sections mapped according to the Lewis’s conformal mapping procedure for a monohull [*Seakeeper* manual]

The inputs of the numerical analyses are similar to *Duhnen*’s experiments output. The five JONSWAP spectra and four speeds were specified in different windows, Table 24. The remote locations are defined conformably to the Figure 19, three positions on the transversal central line, one other in aft starboard and when it is possible one in fore part at port.

	Name	Speed [kts]	Analyse
1	Speed1	5,00	<input checked="" type="checkbox"/>
2	Speed2	10,00	<input type="checkbox"/>

Figure 23 : Operationnal speeds definition [*Seakeeper software*]

The pitch and roll gyradii are obtained from the hull measurement. There are linked to the moment of inertia by the relation (22)

$$k = \sqrt{\frac{I}{m}} \quad (22)$$

with I the moment of inertia [m⁴] roll and pitch and m the displacement of the vessel [kg]. They are expressed in term of percentage of the beam and the length in the software.

Typical values for standard hulls are presented in the Table 8.

Table 8: Typical values of the pitch and roll gyradius [source: *Seakeeper manual*]

	Pitch gyradius [% of length]	Roll gyradius [% of beam]
Monohull	25	35-40

Another characteristic related to the mass and which is used to calculated to roll response of the ship is the vertical centre of gravity.

4.4.2. 2D-linear strip theory, software precisions

The inviscid Salvesen and al. (1970) strip theory without addition damping terms is used to compute the hydrodynamics forces for each transversal 2D-strip. Moreover additional methods are used to specified the method; transom stern, added resistance and wave force, Figure 24.

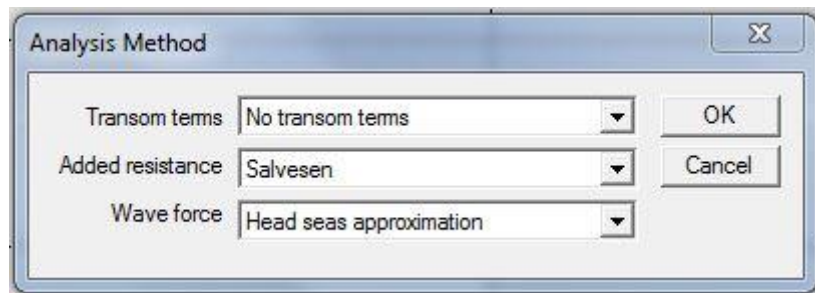


Figure 24 : Choice of analysis methods

- Tansom terms

Our geometries have no transom stern, so there is no additional terms for the coefficients in the motion equations.

- Added resistance

Three methods are proposed to calculate the added resistance of the ship: Salvesen, Gerritsma and Bekelman I and II.

The Salvesen method is accurate for a widely range of hull forms. This method has been chosen to do the analyses. The second-order longitudinal wave force is evaluated to obtain the added resistance. This method is available for head and oblique seas.

- Wave force

The head seas approximation induces simplifications for the wave excitation calculation. It is less time consuming and can be used for heading angle between $160^\circ < \mu < 200^\circ$ to keep a reasonable accuracy. It is an exact method for head seas.

The arbitrary wave heading choice is more time consuming and results have to be analysed with more precautions.

4.4.3. *Postprocessor*

The sectional hydrodynamic coefficients are given in output along with the significant velocities and accelerations for each remote location, the MSI-curves and the spectra.

The MSI-curves are superposed to the severe discomfort boundaries curves (ISO-2631) to get an overall overview of the risks of motion sickness of the ship. This kind of curve cannot be drawn for the *Duhnen* experiment because we only have SVAs.

4.4.4. *Software and strip-theory limitations*

The significant vertical velocity and acceleration are calculated for each remote location defined as inputs. Significant vertical accelerations higher than 0.8g were considered as irrelevant because it is almost equal to the gravitational acceleration and it means that for a person of 90kg will weight alternatively 162kg and 36kg for each waves. It is dangerous!

Lewis’s conformal mapping method

The geometry of the hull is limited in term of measurement by the software due to the Lewis’s conformal mapping method.

Two parameters are introduced to bound available area which can be mapped by this method, the half breadth to draft ratio H_0 and the sectional area coefficient σ_s ,

$$H_0 = \frac{B_s/2}{D_s} \tag{23}$$

$$\sigma_s = \frac{A_s}{B_s * D_s} \tag{24}$$

with B_s the sectional breadth, D_s the sectional draft and A_s the sectional area. The Figure 25 depicted the typical sectional geometries which can be mapped with Lewis’s method according to the half breadth-draft ratios.

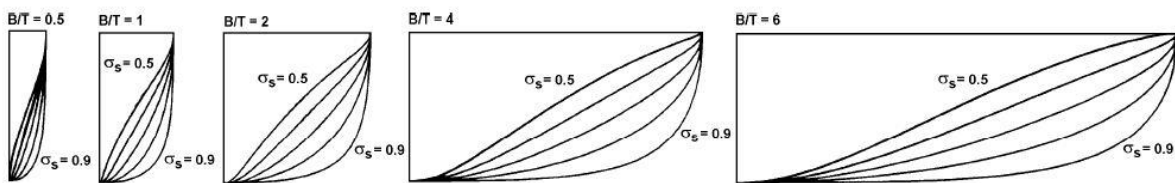


Figure 25 : Typical half breadth ratio mapped by the conformal Lewis’s method

The mapped sections can be check before running the simulation on *Seakeeper*. They are distinguished and coloured differently than the non-mapped cross-sectional areas.

With this method, the hard chines are rounded, the section with low beam/depth ratio are limited. Re-entrant forms and asymmetric forms are not well measured with the two-parameters Lewis transformation, Figure 26.

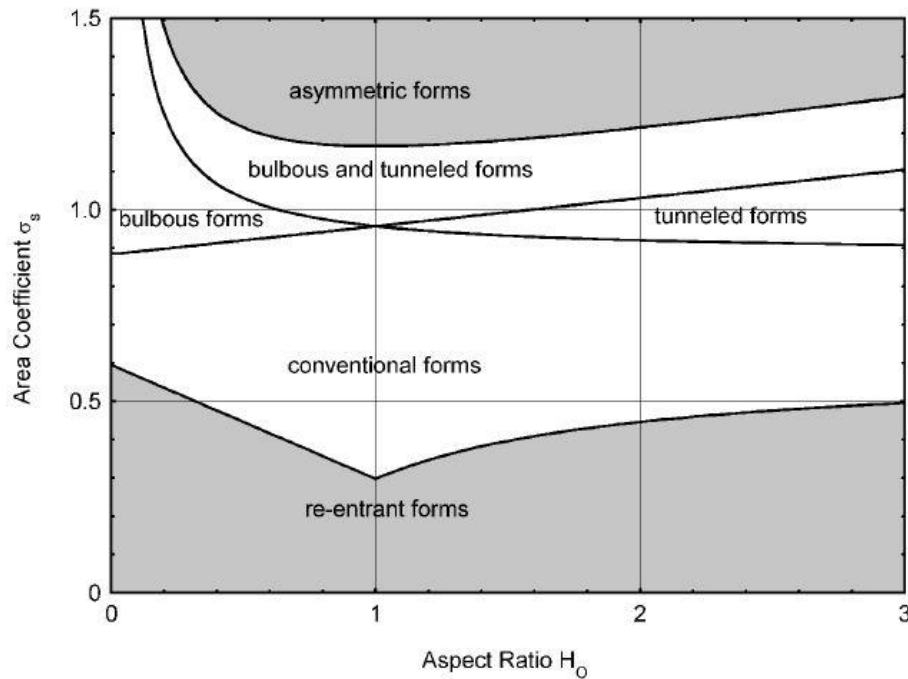


Figure 26 : Range of aspect ratio and area coefficient of Lewis forms [Theoretical manual Seaway – Delft University, report 1216a, February 2001]

Heading angle limitations

The arbitrary heading angle method is not relevant to calculate the MSI in following seas because two or three wave frequencies can have the same encounter frequency. The cosine function presents in the encounter frequency definition (7) is responsible for these characteristic.

Speed limitations

The strip theory is more reliable for Froude number up to 0.8,

$$F_n = \frac{V}{\sqrt{g * L}} \leq 0.8 \quad (25)$$

For the monohull, it means until 14.4km/h, i.e 32.4 knots and 28.2 knots for the catamaran.

4.4.5. Validation of the results

The wave spectrum represents the energy distribution of waves over frequencies. The linear deep water theory supposes that the ship response is linear with the wave amplitude under the assumptions that the speed and the steepness of the waves are limited.

The energy is conserved and the area under the wave spectrum and encounter spectrum curves, called zero spectral moment are similar, Table 9.

of three crew transfer vessels with different hull forms

The aspect of the non-dimensional RAOs curves are also used to validate the simulations. For low encounter frequencies, the wave length is long and the ship “follows” them. The amplitude of the ship response is similar to the wave amplitude, the non-dimensional RAOs is equal to one. For high frequencies, i.e there are many short waves all along the ship length, their effect on the ship motion cancel out and the RAOs tend to zero. The ship is unaffected by the waves. Between this two extreme frequencies, there is a resonance frequency which corresponds to the natural frequency of the vessel. The height of the peak depends on the damping of the associated motion. The heave and pitch resonance amplitude are several times higher than the wave amplitude. The roll resonance amplitude it smaller in comparison to the heave and pitch amplitude. These characteristics have been checked to validate the simulations case by case for monohull and catamaran.

Table 9 : Typical table of *Seakeeper* results (Catamaran – 5 knots – Head seas)

5kn, 5 kts; Head, 180 deg; Spect.5kn (JONSWAP: 5.847 s, 2 m)							
	Item	m0	units	RMS	units	Significant amplitud	units
1	Modal period	5.844	s	--		--	
2	Characteristic wave height	2.000	m	--		--	
3	Spectrum type	JONSWAP		--		--	
4	Wave heading	180.0	deg	--		--	
5	Vessel Speed	5.000	kts	--		--	
6	Vessel displacement	48.781	m^3	--		--	
7	Vessel GMt	15.839	m	--		--	
8	Vessel trim	0.0	deg	--		--	
9	Transom method	No transom term		--		--	
10	Wave force method	Head seas appr		--		--	
11	Added res. method	Salvesen		--		--	
12	Pitch gyradius	6.250	m	--		--	
13	Roll gyradius	9.075	m	--		--	
14	Wave spectrum	0.251	m^2	0.501	m	1.001	m
15	Encountered wave spectrum	0.251	m^2	0.501	m	1.001	m
16	Added resistance	12.297	kN	--		--	
17	Heave motion	0.119	m^2	0.345	m	0.690	m
18	Roll motion	0.00000	deg^2	0.00000	deg	0.00000	deg
19	Pitch motion	10.54	deg^2	3.25	deg	6.49	deg
20	Heave velocity	0.241	m^2/s^2	0.491	m/s	0.981	m/s
21	Roll velocity	0.00000	(Hz)^2	0.00000	Hz	0.00000	Hz
22	Pitch velocity	0.00022	(Hz)^2	0.01495	Hz	0.02989	Hz
23	Heave acceleration	0.565	m^2/s^4	0.752	m/s^2	1.503	m/s^2
24	Roll acceleration	0.00000	(Hz/s)^2	0.00000	Hz/s	0.00000	Hz/s
25	Pitch acceleration	0.00074	(Hz/s)^2	0.02715	Hz/s	0.05431	Hz/s
26	Bow_Amid: Abs. vert. motion	0.446	m^2	0.668	m	1.336	m
27	Bow_Amid: Rel. vert. motion	0.191	m^2	0.438	m	0.875	m
28	Bow_Amid: Abs. vert. velocity	1.157	m^2/s^2	1.076	m/s	2.151	m/s
29	Bow_Amid: Rel. vert. velocity	1.022	m^2/s^2	1.011	m/s	2.022	m/s
30	Bow_Amid: Abs. vert. accel	3.658	m^2/s^4	1.913	m/s^2	3.825	m/s^2
31	Bow_Amid: Rel. vert. accel	10.587	m^2/s^4	3.254	m/s^2	6.507	m/s^2
32	Bow_Amid: Mll slide; tip f/a; tip s/s	0.000	Mll/h	0.000	Mll/h	0.000	Mll/h
33	Bow_P: Abs. vert. motion	0.446	m^2	0.668	m	1.336	m
34	Bow_P: Rel. vert. motion	0.191	m^2	0.438	m	0.875	m
35	Bow_P: Abs. vert. velocity	1.157	m^2/s^2	1.076	m/s	2.151	m/s
36	Bow_P: Rel. vert. velocity	1.022	m^2/s^2	1.011	m/s	2.022	m/s
37	Bow_P: Abs. vert. accel	3.658	m^2/s^4	1.913	m/s^2	3.825	m/s^2
38	Bow_P: Rel. vert. accel	10.587	m^2/s^4	3.254	m/s^2	6.507	m/s^2
39	Bow_P: Mll slide; tip f/a; tip s/s	0.000	Mll/h	0.000	Mll/h	0.000	Mll/h
40	Amidship_S: Abs. vert. motion	0.136	m^2	0.368	m	0.737	m
41	Amidship_S: Rel. vert. motion	0.038	m^2	0.195	m	0.391	m

5. MONOHULL ANALYSIS

5.1. Preliminary design

5.1.1. Design specificities

The high speed monohull has the same displacement than the SWATH. For the same displacement, she will have a longer overall length because the SWATH is more robust.

The design specificities are presented in the Figure 27 and in the next sentences. The fore part of the hull is extended to facilitate the landing (2). The hull is slender with a narrow beam and a sharp bow (1). The sharp bow cuts the waves. The stem has a radius of approximately 1% of the beam to avoid the creation of vortices close to the bow which affect the course stability and reduce the water-plane area. The downward slopping centre line avoids the bow to go out of water (3). The reserve of buoyancy is provided by a higher fore deck (4) and the stern is wide enough to install the machinery equipment (5).

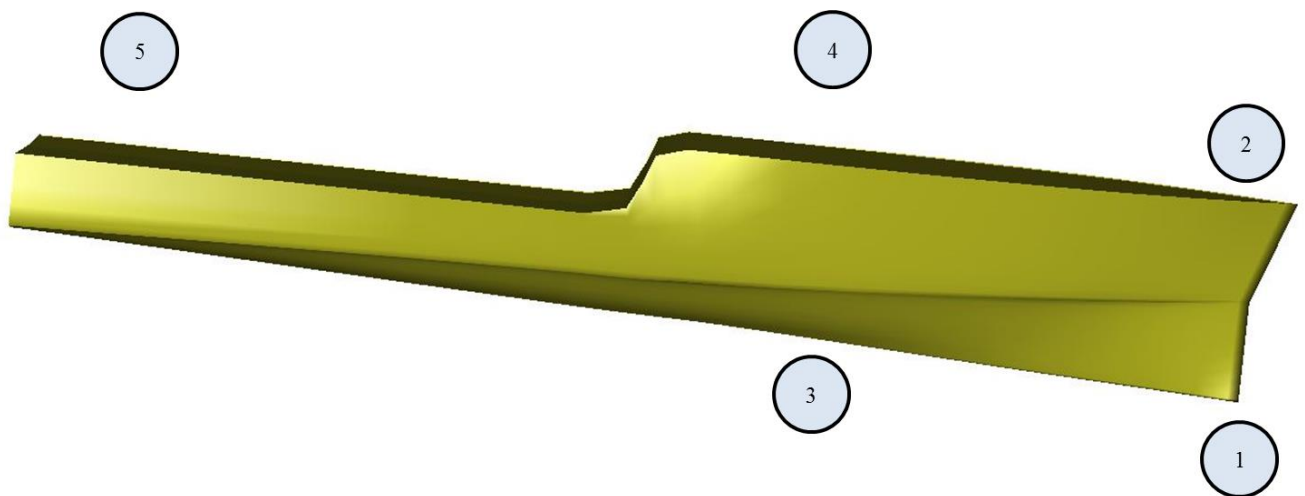


Figure 27 : Design specificities of the monohull

The vertical sides of the bow induce a linear relation between the increasing of the draught and the displaced volume in waves. The response of the ship in waves is more linear. By reducing the non-linear aspect of the hydrodynamic forces, the vertical motion of the hull is less intense.

5.1.2. Similar ships

Comparison of motion sickness incidence
of three crew transfer vessels with different hull forms

The design has been inspired by the three following monohulls, Table 10:

- the Fast Crew Supplier 3507® designed by DAMEN in the Netherlands, (Figure 28, left)
- the 30m crewboat Perez&Deborah von Incat Crowther (Figure 28, right)
- the 33m Veecraft Incat Crew Transfer Vessel.



Figure 28: Comparative monohulls

Table 10 : Characteristics of the comparative ships

	Fast Crew Supplier 3507	30m crewboat Perez&Deborah	33m Crew Transfer Vessel
Shipyard	DAMEN	Incat Crowther	Veecraft Incat
Hull length [m]	35.92	30.0	33.0
Lenght overall [m]	35.92	29.0	30.3
Beam [m]	7.35	7.0	7.5
Draft [m]	2	1.49	
Depth [m]	3.30 from sides		
Crew	6	6	8
Industrial personnel	29	30	100
Material construction	Aluminium	Aluminium	
Main engine	3x CAT C32 ACERT	3x CAT C32 ACERT	3 x KTA5
Propulsion	3 fixed pitch propellers	3	3 x propellers
Cruise speed [kn]		25	
Max speed [kn]	29	30	
Generators [kW]	2 x 69kW Caterpillar C 4.4 TA	2x50kW	
Fuel tanks	34.90 m ³	2x10 000 L	36 000 L
Fresh water cargo	24.90 m ³	10000 L	1 000 L
Grey water	1.30 m ³	3 000 L	
Dirty oil	0.50 m ³		
Deck tanks	2 x 5.00 m ³		
Deck cargo area [sqm]	120	50	
Deck strength [t/sqm]	1.4	1.5	
Deck cargo [t]	168	75	70

The main characteristics of the monohull are presented in the Table 11.

Table 11 : General geometric characteristics of the monohull

Length overall	32.9 m
Beam overall	6.6 m
Depth at sides	3.3 m
Draught max	2.0 m
Max. speed	29 kn
Main engines	3 x C32 C TTA caterpillar
Crew	6 persons
Industrial personnel	29 persons
Fuel oil	35 m ³
Fresh water cargo	25 m ³
Sea area (BV classification)	3

5.1.3. Hydrostatics

Two load cases have been studied, Table 12 during the design phase. The first one concerns the “go offshore” way, when the monohull has the same displacement than the SWATH, 126 tonnes. The draft is equal to 2.0 meters. When the vessel comes back from the offshore installations, she is lighter with a draft a 1.8 meter draft and 91.5 tonnes of displacement. The second load case is called “go home”. The metacentric height is greater when the ship goes home because the VCG is lower.

Comparison of motion sickness incidence
of three crew transfer vessels with different hull forms

Table 12 : Hydrostatics of the monohull [*Hydromax* analysis]

	"Go offshore"	"Go home"	
	T = 2,0 m	T=1,75 m	T = 1,80 m
Displacement tonne	126.0	87.8	95.2
Heel to Starboard degrees	0.0	0.0	0.0
Draft at FP m	2.0	1.7	1.8
Draft at AP m	2.0	1.8	1.8
Draft at LCF m	2.0	1.8	1.8
Trim (+ve by stern) m	0.0	0.0	0.0
WL Length m	32.0	32.0	32.0
WL Beam m	6.6	6.6	6.6
Wetted Area m ²	197.1	174.6	179.7
Waterpl. Area m ²	154.8	143.8	146.9
Prismatic Coeff.	0.8	0.8	0.8
Block Coeff.	0.3	0.2	0.2
Midship Area Coeff.	0.6	0.6	0.6
Waterpl. Area Coeff.	0.7	0.7	0.7
LCB from amidsh. (+ve fwd) m	-2.7	-2.4	-2.5
LCF from amidsh. (+ve fwd) m	-3.2	-3.7	-3.6
KB m	1.5	1.4	1.4
KG m	2.5	2.1	2.1
BMt m	3.4	4.2	4.0
BML m	78.8	103.2	97.0
GMt m	2.4	3.4	3.3
GML m	77.8	102.5	96.3
KMt m	4.9	5.5	5.4
KML m	80.3	104.6	98.4
Immersion (TPc) tonne/cm	1.6	1.5	1.5
MTc tonne.m	3.1	2.8	2.9
RM at 1deg = GMt.Disp.sin(1) tonne.m	5.3	5.2	5.5
Max deck inclination deg	0.0	0.0	0.0
Trim angle (+ve by stern) deg	0.0	0.0	0.0

5.1.4. Lines plan

The general monohull form is depicted by her lines plan in the Figure 29.

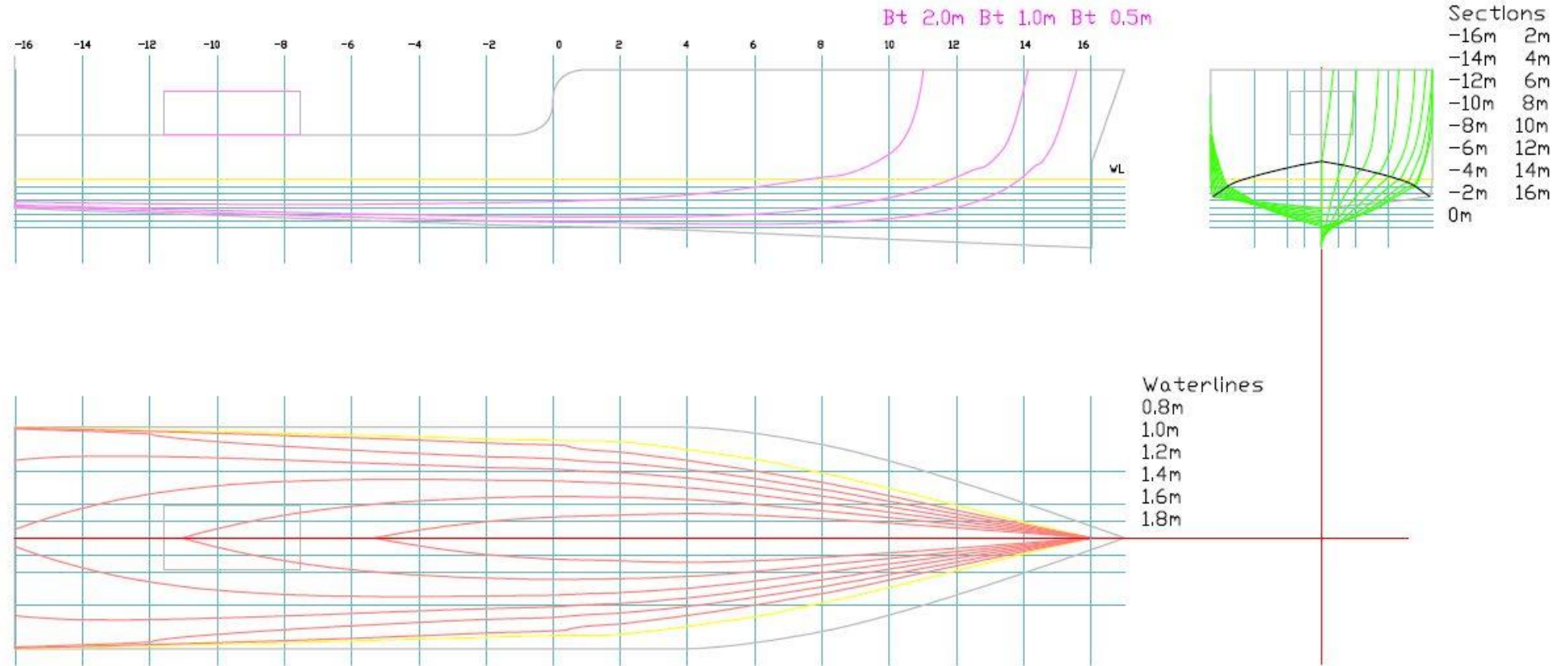


Figure 29 : Lines plan of the 33m monohull

5.1.5. Structural weight

Estimation of weight and centre of gravity is an essential task in the design phase of a vessel, and the quality of this work will be crucial for the success of the project. The weight and centre of gravity will be refined throughout the project. For each loop of the design spiral, Figure 30 the weight will be more accurate until obtaining the final values.

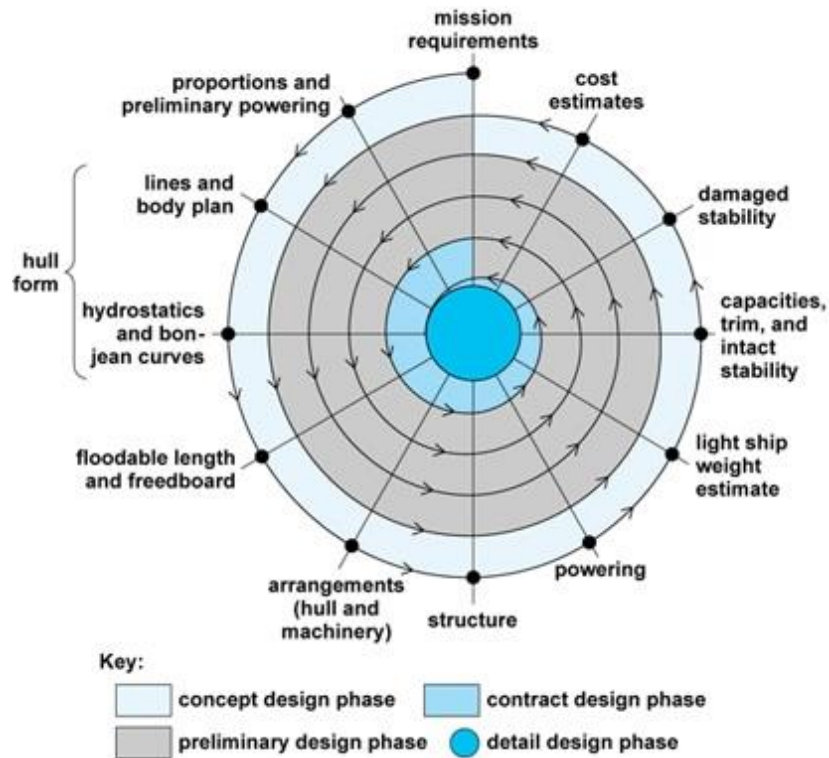


Figure 30 : Spiral design of ship [www.marinewiki.org, 17/12/13]

Seakeeper automatically defines the longitudinal position of the centre of gravity aligned with the centre of buoyancy. The purpose of the weight estimation is mainly to determine the vertical position of the centre of gravity.

One manner to calculate the structural weight during the preliminary stage of the design is by following the Grubisic's method [6]. Grubisic established series of relations based on two databases composed of respectively 34 fast vessels with the total weight breakdown known and 142 small fast crafts for which only the lightship weight was known. The overall length of the vessels is up to 60 meters.

The monohull can be included into this set because her maximum sustained speed satisfies the following equation [3]:

$$v > 3.7 * \nabla^{0.1667} m/sec \quad (26)$$

with ∇ the volume displacement.

The calculations for the structural weight are exposed in Annex 1.

The Grubisic method gives a range for the structural weight, Table 13.

Table 13 : Estimation of the structural weight according to Grubisic

	Structural weight [t]
Estimation	42.43
+13%	47.95
-13%	36.92

A refinement has been done according to Dubrovsky [7], the structural weight of a similar monohull is 25 to 30% lighter than her comparative SWATH, Table 14.

Table 14 : Weight structure comparison between the SWATH and a similar monohull

	Structural weight (t)
25.2m SWATH	41.5
30% lighter	29.05
25% lighter	31.125

A 3D-model of the hull has been built on *Inventor* by considering the main structural elements defined by Grubisic to determine the vertical position of the centre of gravity of the hull and superstructure, Figure 31. The position of the bulkheads and the thickness of the main plates were established according to the Bureau Veritas rules [8]. The calculi are also exposed in the Annex 1.

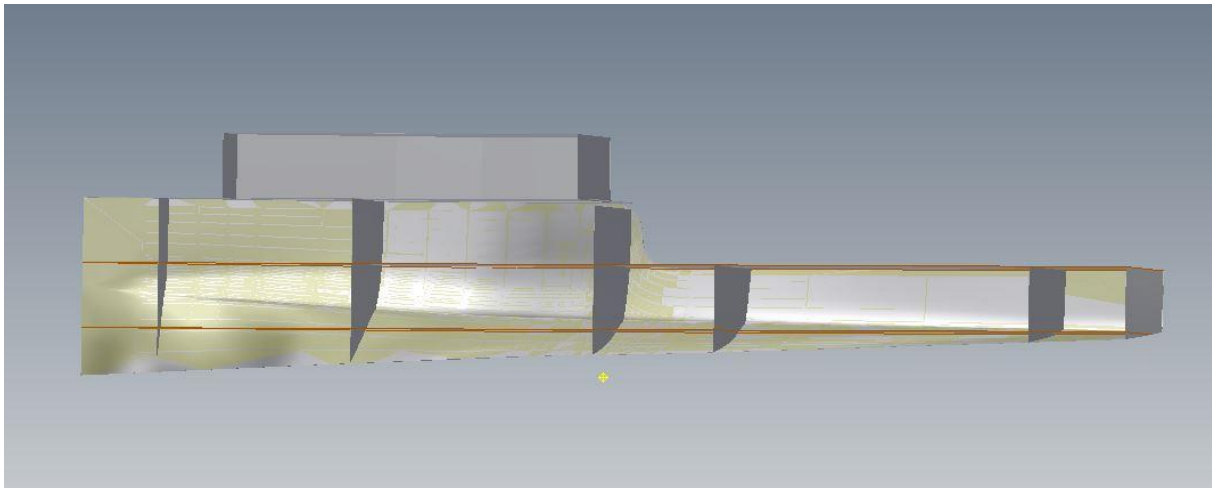


Figure 31 : Preliminary structure of the monohull

The metacentric height is related to the geometry of the ship, a narrow and deep hull has a high metacentric height. A similar “traditional” hull and the SWATH will have the same metacentric height but in this case, the hull is not conventional but narrower than a conventional monohull, so the metacentric height of the axe bow hull will be higher than the SWATH.

5.3.2 Lightship weight

The structural weight has been fixed to 31.1 tonnes to carry out the analyses. A preliminary weight estimation was conducted to estimate the position of the centre of gravity of the lightship, Table 15 and Table 16.

The sets of elements corresponding to the heaviest parts of the ship weight were considered for the weight estimation. The weight of the elements of the living crew area is the same for all the ships, values from SWATH weight estimation were used.

Table 15 : Weight of the sets

	Weight [t]	LCG [m]	TCG [m]	VCG [m]
Structure + superstructure	31.13448	-0.348	0	2.78240862
Engine room set	19.66	-11.238	0	1.8
Crew living area set	2.6	3.75	0	1.8
Main deck room set	1.5	6.5	0	5.2

Table 16 : Lightship weight estimation and centre of gravity

	Weight [t]	LCG [m]	TCG [m]	VCG [m]
Lightship	58.418	-3.498	0	2.452

The permanent ballast are not included into the lightship weight, they are defined in the *Hydromax* table, “permanent b1” and “permanent b2” in Table 17.

5.3.3 Tanks definition

The position of the tanks have been defined with *Hydromax*, Table 17.

The load case specificities are:

- “Go offshore” – Ship full loaded with cargo, crew and passengers,
- “Go home” – Half of the fuel, 50% of the fresh water, crew and passengers, no cargo.

The “go offshore” load case has been used to compared the seasickness.

Table 17 : Tanks definition

	Relative density	Fluid type	Aft [m]	Fore [m]	F Port [m]	F Starboard [m]	F Top [m]	F Bottom [m]
FW1	1	Fresh Water	0.9	5.4	1.5	3	3.3	1.4
FW2	1	Fresh Water	0.9	5.4	-3	-1.5	3.3	1.4
Fuel.Star	0.9443	Fuel Oil	-3.7	0.9	1	3	3.2	0
Fuel.Port	0.9443	Fuel Oil	-3.7	0.9	-3	-1	3.2	0
Lub.Oil	0.92	Lube Oil	-5.5	-3.7	0	1	1.4	0
Dirty Oil	0.92	Lube Oil	-5.5	-3.7	-1	0	1.4	0
Grey water	1.025	Water Ballast	9.3	12.7	-2.5	1	1	0
Deck tank	1.025	Water Ballast	-11.5	-7.5	-1	1	4.6	3.349
Ballast1	1.025	Water Ballast	0.9	5.4	0	3	1.4	0
Ballast2	1.025	Water Ballast	0.9	5.4	-3	0	1.4	0
bilge	1.025	Water Ballast	-8	-6	-1	1	1.4	0
permanent b1	1.025	Water Ballast	-16	-14	2	3.5	2	0
permanent b2	1.025	Water Ballast	-16	-14	-3.5	-2	2	0

5.1.6. General arrangement

The rough general arrangement of the ship is presented in the Figure 32 and Figure 33. The main deck is composed of passenger's room with sufficient seats for 30 people, a luggage room, toilets and the wheelhouse in the fore part of the deck. Two tanks for cargo are located in the aft part of the main deck. The navigation room is located at the first floor of the wheelhouse.

The machine room is located at the below deck along with the crew living area which can welcome 6 crew members.

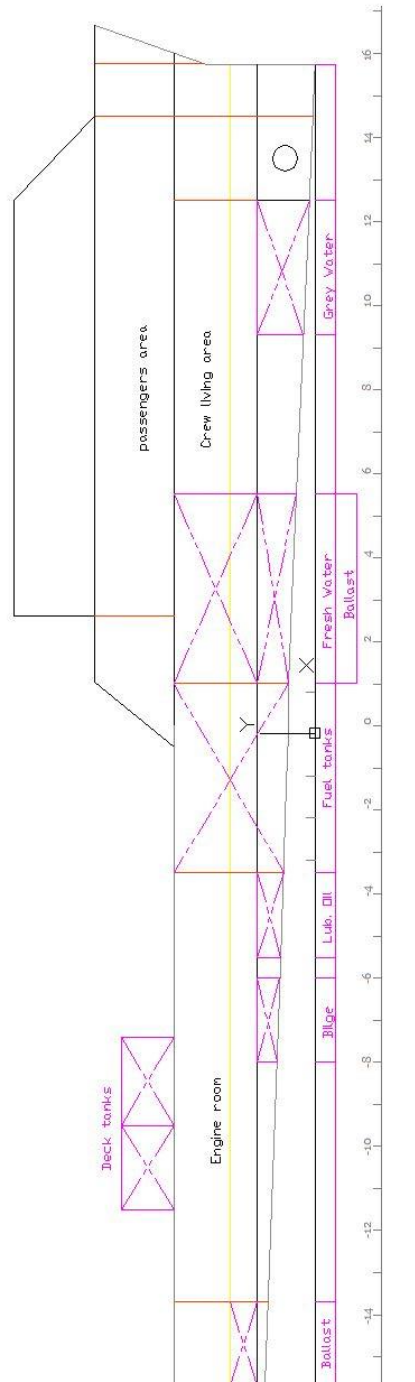


Figure 32: General arrangement of the monohull (profile view)

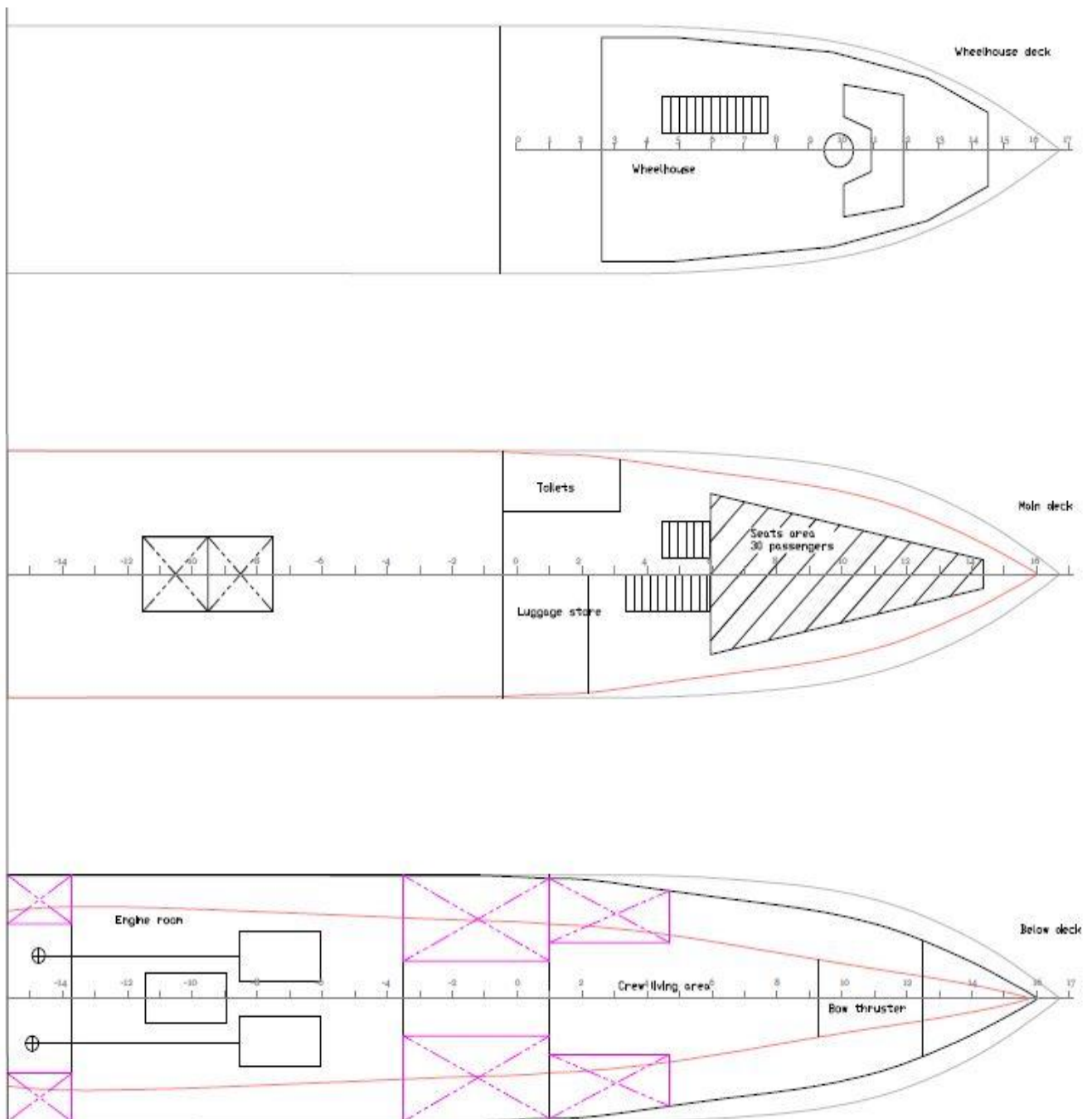


Figure 33: General arrangement of the monohull (deck views)

5.1.7. Vertical position of the centre of gravity

The position of the centre of gravity has been established for the two load cases. There are presented in the Table 18 and Table 19.

Table 18 : Weight balance of the "Go offshore" load case

	Quantity (1=100%)	Sounding pipe [m]	Weight [t]	LCV [m]	TCG [m]	VCG [m]
FW1	1	10.264	10.264	3.043	-2.153	2.488
FW2	1	10.264	10.264	3.043	2.153	2.488
Fuel.Star	1	15.695	15.695	-1.414	1.899	2.268
Fuel.Port	1	15.695	15.695	-1.414	-1.899	2.268
Lub.Oil	1	0.87	0.87	-4.586	0.467	1.134
Dirty Oil	0	0.87	0.009	-4.234	-0.093	0.798
Grey water	0	1.369	0.014	11.668	0	0.25
Deck tank	1	9.548	9.548	-9.541	0	3.974
Ballast1	0	4.105	0	3.124	0.662	1.099
Ballast2	0	4.105	0	3.124	-0.662	1.099
bilge	1	1.874	1.874	-6.979	0	1.168
permanent b1	1	1.42	1.42	-15.008	2.584	1.72
permanent b2	1	1.42	1.42	-15.008	-2.584	1.72
Total loadcase			125.49	-2.685	0.003	2.482

Table 19 : Weight balance of the "go home" load case

Go home						
	Quantity (1=100%)	Sounding pipe [m]	Weight [t]	LCV [m]	TCG [m]	VCG [m]
FW1	0.1	10.264	1.026	2.873	-1.833	1.618
FW2	0.1	10.264	1.026	2.873	1.833	1.618
Fuel.Star	0.5	15.695	7.847	-1.429	1.798	1.788
Fuel.Port	0.5	15.695	7.847	-1.429	-1.798	1.788
Lub.Oil	0.2	0.87	0.174	-4.531	0.336	0.909
Dirty Oil	1	0.87	0.87	-4.586	-0.467	1.134
Grey water	1	1.369	1.369	10.849	0	0.739
Deck tank	0	9.548	0	-9.541	0	3.974
Ballast1	1	4.105	4.105	3.124	0.662	1.099
Ballast2	1	4.105	4.105	3.124	-0.662	1.099
bilge	1	1.874	1.874	-6.979	0	1.168
permanent b1	1	1.42	1.42	-15.008	2.584	1.72
permanent b2	1	1.42	1.42	-15.008	-2.584	1.72
Total loadcase			91.503	-2.632	-0.004	2.108

5.1.8. Conclusion

The vertical position of the centre of gravity is equal to 2.48m when the vessel goes offshore and 2.1m when she goes back without cargo, at the end of the day.

5.2. Numerical model used for the monohull analysis

5.2.1. Hull measurement

The hull was split into 200 transversal sections and the conformal mapping was checked in the bow region to be sure that the axe-bow was taken in consideration during the analysis. The software takes in consideration only the underwater part of the hull to compute the seakeeping analysis.

The monohull has a smaller roll gyradius due to the specific form of the hull, Figure 34. The range of roll gyradius is 35-40% of the beam overall for conventional hull form.

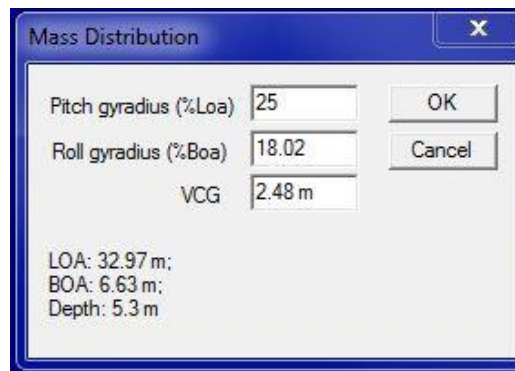


Figure 34 : Roll and pitch gyradii of the monohull

One of the assumptions of the linear strip theory is that the fluid is inviscid. A part of the viscous effect of the fluid is neglected by the initial assumptions in the prediction of the roll response motion. *Seakeeper* proposes to add non-dimensional additional roll damping coefficient separately. The additional roll damping coefficients were computed for each speed according to the Ikeda's theory. It is a simple prediction formula to improve the prediction of roll motion response in strip method.

5.2.2. Inputs data

A range of 91 frequencies around the JONSWAP modal frequency were used to do the simulation.

The JONSWAP wave spectrum is defined with two parameters, the significant wave height and the wave frequency, Table 20.

Table 20 : JONSWAP spectra definition from the *Duhnen* experiments

Speeds	Significant wave height [m]	Modal frequency [hz]
5	2	0.171
8	2.4	0.171
10	2	0.146
12	1.5	0.207
	2.4	0.127

The positions of the remote locations are depicted in Figure 35: two remote locations in the fore part of the ship, in the passenger room and two at the stern.

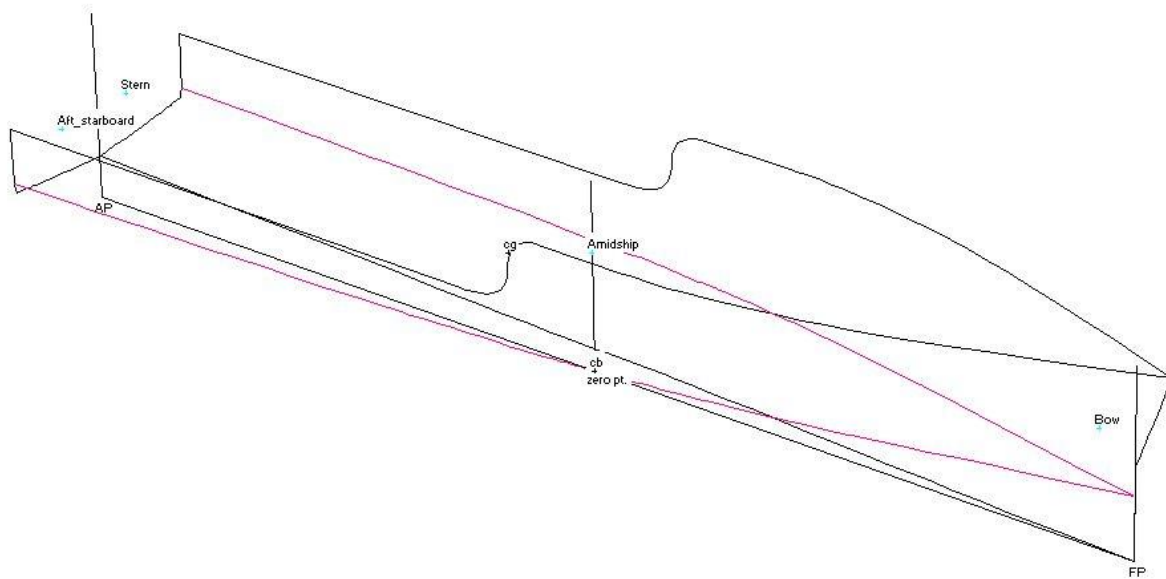


Figure 35 : Position of the remote locations

Two series of simulations were conducted, one for the head seas approximation and the other with the arbitrary wave method to calculate the excitation wave forces.

5.2.3. Results and MSI-curves

Some tools are drawn on the graphics to facilitate the interpretation of the results such as the tendency curves (logarithmic $a \cdot \ln(x) + b$ or linear $ax + b$ form).

Moreover three regimes are presented in the curves:

- during the first minutes, the MSI—curve skyrockets, it is called regime 1
- there is a transition period where the curve inches up, it is called regime 2
- finally, the stagnation period when the curve regime a threshold value, regime 3

The three regimes are separated by vertical black dotted lines for the worst MSI-curves in the Figure 37 and Figure 38 for the monohull and Figure 45 and Figure 46 for the catamaran.

Worst location on bridge in term of motion sickness

The maximum SVA and their location on the bridge along with the peak frequency of the ship response are given in the Table 21.

Table 21 : Results for the 5 and 10 knots simulation between the Monohull and SWATH (peak encounter frequencies)

	Peak frequency [Hz]	Max. significant vertical acceleration [g]	Location of the bridge
2705000	0.125	0.080	Aft S - BV5
2705090	0.168	0.128	Aft S - BV5
2705135	0.192	0.148	Aft AM - BV4
2705180	0.180	0.142	Aft AM - BV4
2705315	0.151	0.073	Aft S - BV5
M05000	0.124		Bow
M05090	0.171	0.335	Aft
M05135	0.201	0.531	Bow
M05180	0.234	0.464	Bow
M05315	0.137	0.191	Aft S
2710000	0.196		Aft
2710090	0.196	0.120	Aft
2710135	0.204	0.160	Aft AM - BV4
2710180	0.201	0.160	Aft
2710315	0.151	0.060	Aft S - BV5
M10000	0.069		Bow
M10090	0.138	0.272	Aft
M10135	0.201	0.599	Bow
M10180	0.217	0.588	Bow
M10315	0.096	0.433	Aft S

The worst location of the significant vertical acceleration of the SWATH is the aft part of the ship because the vertical localization is on top vertical of the propeller (additional inertia) which goes up the discomfort on board. For a monohull, the maximum vertical acceleration is in the bow region, Figure 20.

Spectra differences

The JONSWAP spectra are a little bit different between the 5 and 10 knots tests which have been conducted the same day but the morning and the afternoon, Figure 36.

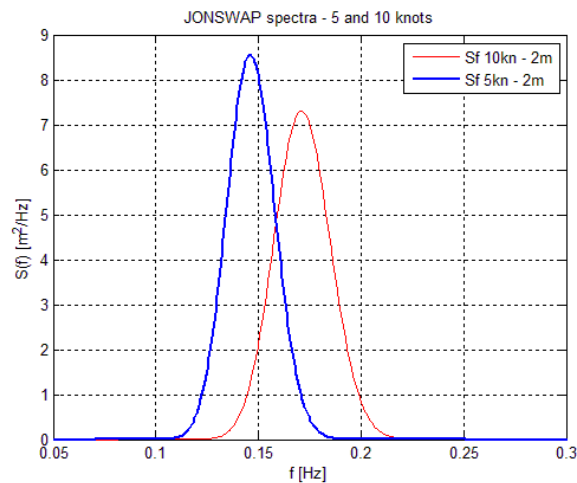


Figure 36 : JONSWAP spectra for the 5 and 10 knots tests

The peak frequency was higher during the 10 knots measurement, the wave period were longer, Figure 36. The peak encounter frequencies are shorter for the 5 knots experiments and then the resonance period longer. The sensibility of SWATH to waves should be less than monohull, the MSI-curves difference between 5 and 10 knots for same heading angles are less pronounced than the monohull.

The MSI-curves comparisons for 5 and 10 knots speed are depicted in the Figure 37

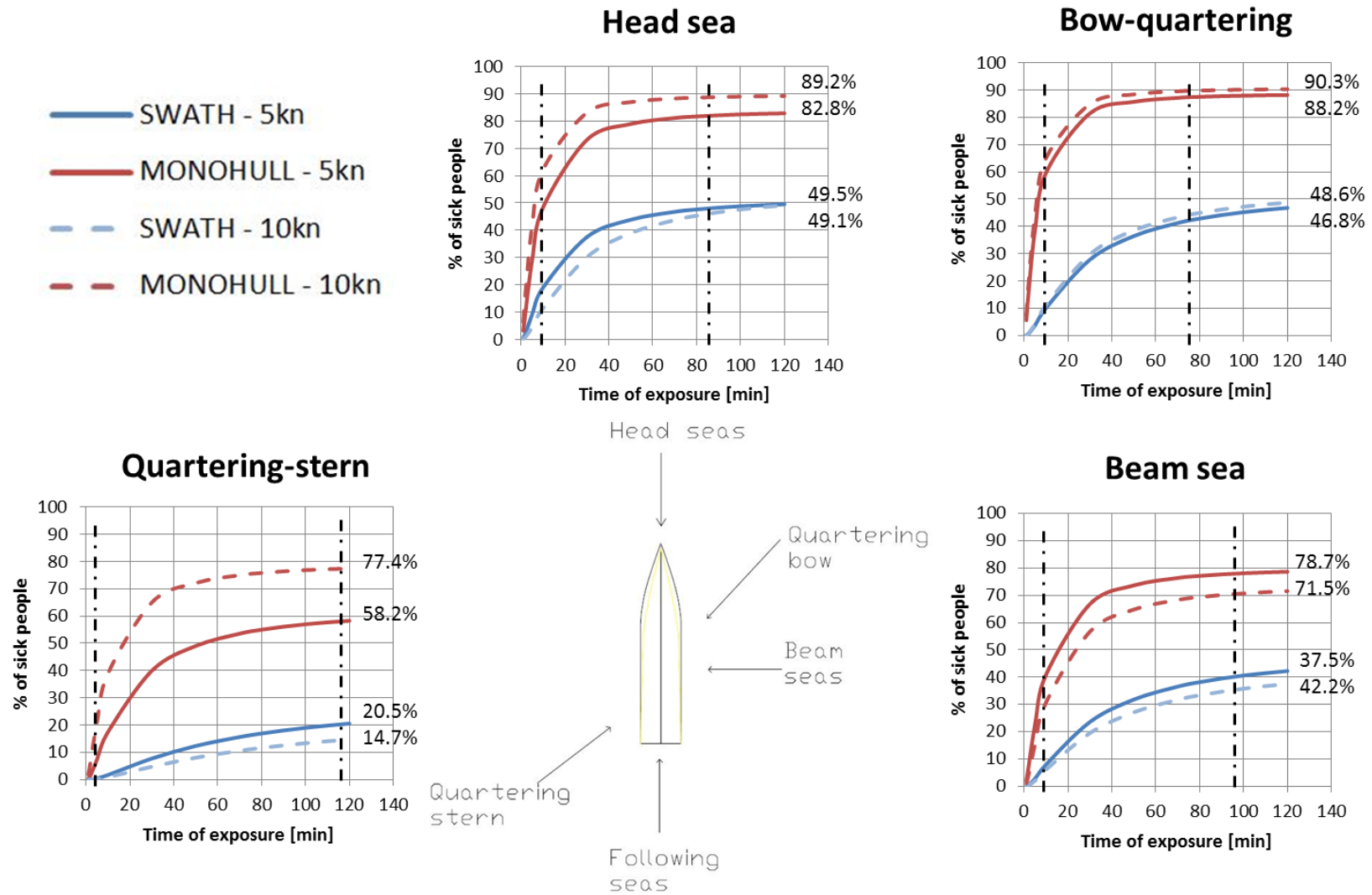


Figure 37 : MSI-curves comparison between the monohull and the SWATH for 5 and 10 knots speed

Comparison between Monohull and SWATH at 5 and 10 knots

People are more seasick on monohull than on SWATH. Moreover waves from stern, from 90° to 270° induce less motion sickness than waves which encounter the ship by the bow. The seakeeping behaviour of the monohull is better in in stern-quartering seas where 30% of the passengers will be sick in 20 min instead of 50% in beam seas.

Table 22 : Difference in term of percentage of seasick people on board after 10, 50 and 120 minutes on board

Heading angle [°]	Time of exposure [min]	Difference Monohull vs SWATH	
		% of sick people at 5 knots	% of sick people at 10 knots
90°	10	5.2	5.1
	50	2.3	2.4
	120	1.9	1.9
135°	10	5.9	6.1
	50	2.4	2.3
	120	1.9	1.9
180°	10	2.6	5.7
	50	1.8	2.3
	120	1.7	1.8
315°	10	10.4	13.4
	50	4.0	4.9
	120	2.8	3.4

The difference of seasick people is significant during the ten first minutes on board, people are 3 to 10 times sicker on monohull than SWATH (regime 1). It is also represented by the coefficient *a* of the logarithmic trend curves, Table 23. After one hour, there are two times more people sick on the monohull in beam seas, bow quartering and head seas than SWATH. In stern-quartering waves (315°), the difference is higher because the monohull is more heeled by the waves. The SWATH is less sensitive due to her longer natural rolling period. These characteristics are also presented in the Table 23.

Table 23 : Evolution of MSI curve through tendency curves

Test	Tendency curve equation	Coefficient R ²
Monohull 5kn	$17.62 \cdot \ln(x) - 0.85$	0.98
SWATH 5kn	$10.12 \cdot \ln(x) - 7.58$	0.95
Monohull 10kn	$16.60 \cdot \ln(x) - 4.64$	0.98
SWATH 10kn	$8.94 \cdot \ln(x) - 7.13$	0.94

The SWATH trend curves have lower correlation coefficient, there are less accurate than the trend curves of the monohull.

The results for the 8 and 12 knots tests are presented in the Figure 38. The encounter frequency is expressed in Hertz.

.

of three crew transfer vessels with different hull forms

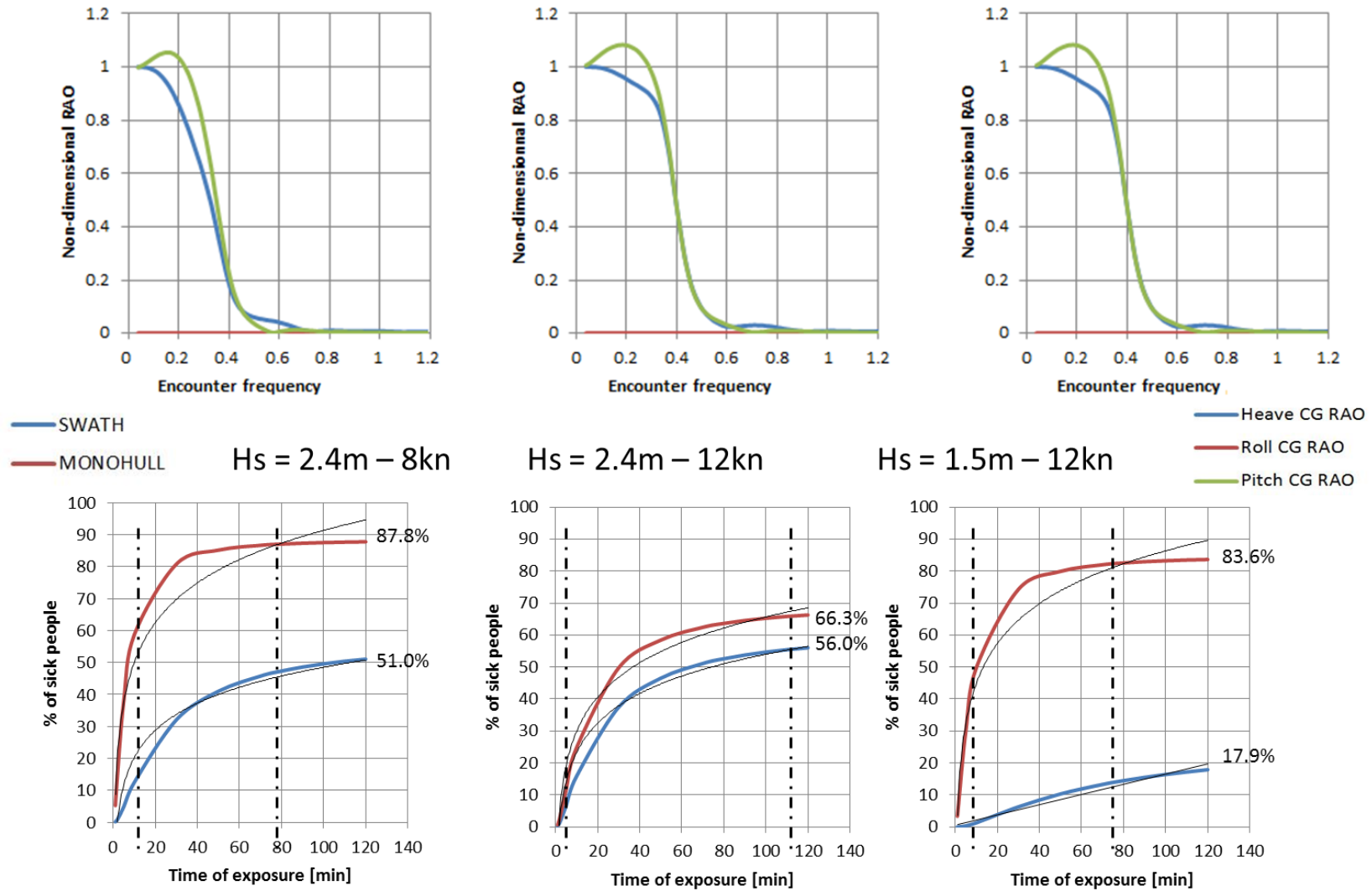


Figure 38 : Monohull RAO and MSI-curves comparison with the *Duhnen* Master Thesis developed at West Pomeranian University of Technology, Szczecin

The non-dimensional RAOs have the same form because the three tests are defined with head seas. For long waves (low frequencies), the ship follows the waves and then the ship motion amplitude has the same order of magnitude than the wave amplitude. The RAOs tend to unit. The ship does not “see” short waves which are really short in comparison to her length, then the ship motion response tends to zero and the RAOs also. The *Seakeeper* software considers that the waves are unidirectional, in head seas. There is no rolling response. The red curve is equal to zero in the Figure 38.

Table 24 : Tendency curve equations of the MSI-curves comparison between SWATH and Monohull at 8 and 12 knots

Input datas	Ship type	Tendency curve equations	R ²
8kn - 2.4m - 180°	SWATH	$12.25*\ln(x)-7.95$	0.96
	Monohull	$17.92*\ln(x)+8.78$	0.96
12kn - 2.4m - 180°	SWATH	$13.41*\ln(x)-7.80$	0.97
	Monohull	$15.63*\ln(x)-6.31$	0.98
12kn - 1.5m - 180°	SWATH	$0.16*x+0.4264$	0.97
	Monohull	$17.99*\ln(x)+3.45$	0.97

The coefficient “a” of the tendency curves, Table 24 is higher in the case of the monohull, the percentage of sick people on board is increasing faster.

Table 25 : Comparative table of the results from the Bremen’s Hochschule and the comparative monohull

	Peak frequency [Hz]	Max. significant vertical acceleration [g]	Location of the bridge
HB008180	0.127	0.167	Aft starboard
HB012180	0.207	0.192	Aft starboard
HB112180	0.127	0.071	Front*
M008180	0.165	0.486	Bow
M012180	0.373	0.542	Stern
M112180	0.186	0.413	Bow

For the third test at 12 knots with a significant wave height of 1.5m, the SVAs were given only for the two accelerometers in the fore part of the *Duhnen*. The response of the monohull during the second test (2.4m – 12kn -180°) is irrelevant for the SVA at the bow because it is higher than 1g. For small wave height, the seasickness difference between monohull and SWATH is higher because the SWATH has a lower metacentric height than the monohull.

6. CATAMARAN ANALYSIS

6.1. Preliminary design

6.1.1. Similar ships

The small catamaran represent 80% of the fleet of crew transfer vessels dedicated to offshore wind farms. There are many shipyards which have developed a special branch dedicated to the offshore wind farms vessels. The similar vessels which were used during the design phase of the project come from three shipyards, Damen, Marine Craft and SeaZip. The three ships are derived from the same catamaran, which is the *Damen FCS 2610*, first column of the Table 26.

Table 26 : Characteristics of the comparative catamaran

	MCS Sirrocco/MCS Pampero	High speed support vessel [®] 2610 "HSSV 2610"	SeaZip 1 / SeaZip 2
Shipyards	DAMEN	Owner MARINECO	SeaZip Offshore service
Lenght overall [m]	25.75	26.2	25.75
Beam [m]	10.4	10.4	10.4
Draft [m]	2.2 max	1.15-1.45	2.2 max
Depth [m]			2.9m at sides
Displacement	80 tonnes (50% consumables)		72.8 (lightsip)
GRT	81.58		147
Crew		4	4
Industrial personnel	14 with crew	12	12
Material construction	aluminium	aluminium	aluminium
Main engine	2x C32 TTA	2x C32 TTA B	2x C32 TTA B
Total power [bkW]	1800	1790	2x 895 kW
Gearbox	Reintjes ZWVS 440/1	Reintjes ZWVS 440/1	Reintjes ZWVS 440/1
Propellers	Fixed-pitch propellers	Fixed-pitch propellers	Fixed-pitch propellers
Bow thruster	2x 50kW	2x 51kW	2x 44W
Cruise speed [kn]	22	22	25 average speed
Max. speed [kn]	26	26	
Main generator set	2x Caterpillar C2.2T	1x Caterpillar C2.2 T	2x Caterpillar C2.2
Generator capacity	2x34 kVA, 50Hz, 230/400V	22.5 kW / 28.0 kVA	22.5 kW / 28.0 kVA
Fuel tanks [m ³]	14.2	20	14.2 to 22.2 (with ballast)
Fresh water tanks [m ³]	1.8	2	2
Grey water [m ³]		0.3	0.5
Bilge [m ³]			0.33
Ballast [m ³]			8 - fuel oil (trim)
Dirty oil [m ³]	0.33		
Deck cargo [t]		15	5 to 15
Deck cargo area [m ²]	90	90	90
Max deck strength [t/m ²]	1.5	1.5	1.5
Deck crane	Heila HLM 20-2s Capacity 2.2t@8.5m	Heila 20-2s Capacity 2.2t@8.6m	SWL 2.2t@8.6m

The hull of the catamaran is an axe-bow with the characteristics presented in Table 27.

Table 27 : Main characteristics of the catamaran

Length overall	25.0m
Waterline length	23.4m
Beam overall	13.0m
Maximum draft	2.7m
Gross tonnage	225.0
Max. Speed	18 kn
Full loaded displacement	126 t
Spacing of CL demihulls	7.0m

6.1.2. Hydrostatics

The study has been done for the full load case condition, with a draft of 2.15m, Table 28.

Table 28 : Hydrostatics of the catamaran – full loaded load case condition

	Draft [m]		
	2.1	2.15	2.2
Displacement tonne	93.17	99.83	106.5
Heel to Starboard degrees	0	0	0
Draft at FP m	2.1	2.15	2.2
Draft at AP m	2.1	2.15	2.2
Draft at LCF m	2.1	2.15	2.2
Trim (+ve by stern) m	0	0	0
WL Length m	25	25	25
WL Beam m	10.545	10.561	10.576
Wetted Area m ²	203.872	209.331	214.793
Waterpl. Area m ²	129.507	130.38	131.252
Prismatic Coeff.	0.844	0.839	0.834
Block Coeff.	0.239	0.249	0.258
Midship Area Coeff.	0.683	0.709	0.737
Waterpl. Area Coeff.	0.715	0.716	0.716
LCB from amidsh. (+ve fwd) m	-1.238	-1.325	-1.401
LCF from amidsh. (+ve fwd) m	-2.544	-2.544	-2.544
KB m	1.686	1.715	1.744
KG m	2.971	2.971	2.971
BMt m	18.301	17.178	16.188
BML m	57.747	54.275	51.212
GMt m	17.015	15.922	14.961
GML m	56.461	53.019	49.985
KMt m	19.986	18.893	17.932
KML m	59.432	55.99	52.956
Immersion (TPc) tonne/cm	1.327	1.336	1.345
MTc tonne.m	2.104	2.117	2.13
RM at 1deg = GMt.Disp.sin(1) tonne.m	27.667	27.739	27.815
Max deck inclination deg	0	0	0
Trim angle (+ve by stern) deg	0	0	0

6.1.3. Lines plan

The lines of the catamaran depicted in Figure 39 have been drawn on *Maxsurf* and imported on *AutoCad 2013*.

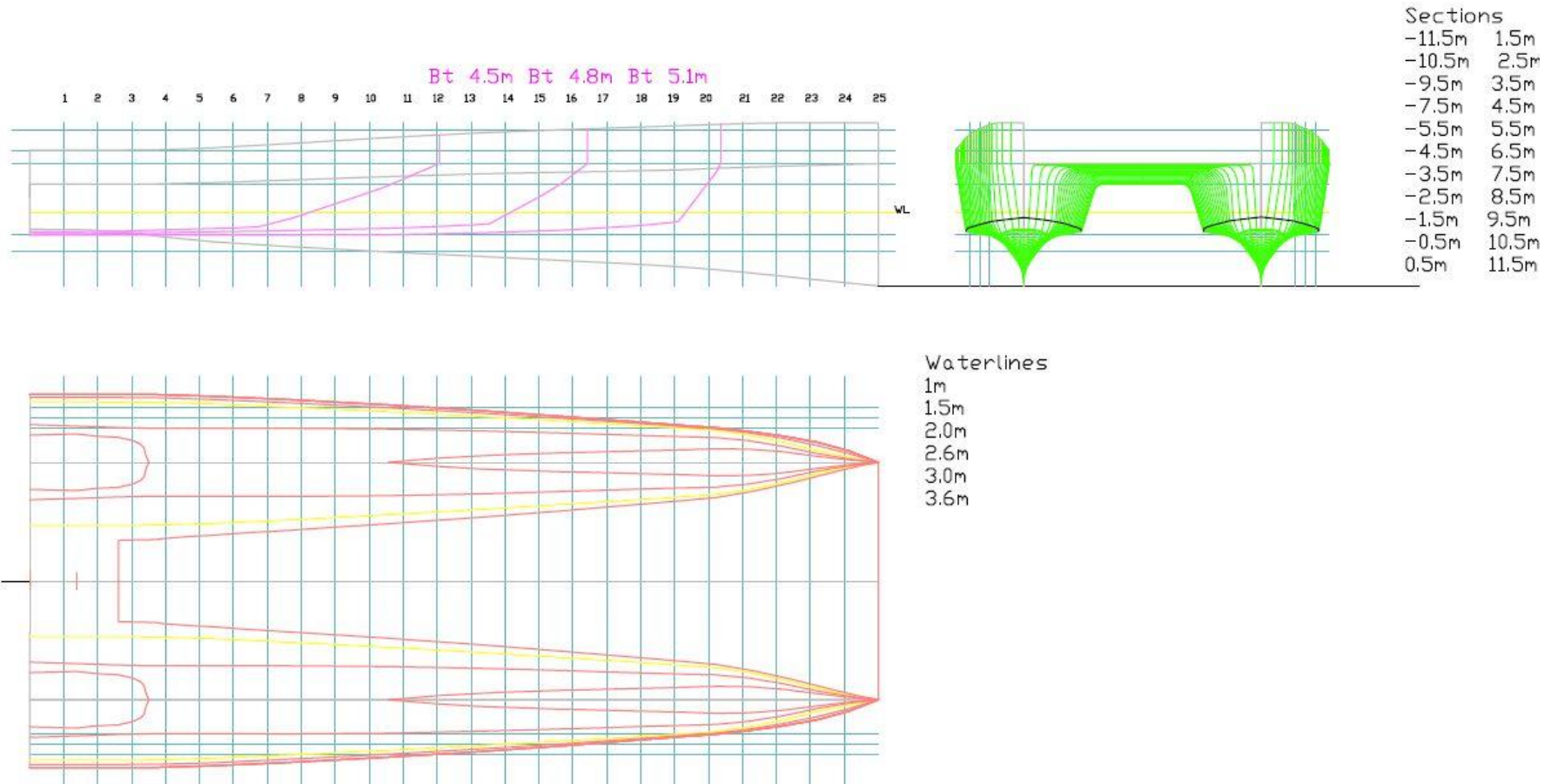


Figure 39 : Lines plan of the 25m-catamaran

6.1.4. Structural weight

The structure of the catamaran has been designed according to the GL classification rules for high-speed craft. Rules for offshore service vessels have been published in 2012. They specified the rules to use for specific craft using in the offshore industry such as the crew boats. There are 16 categories of crew boats, Figure 40.

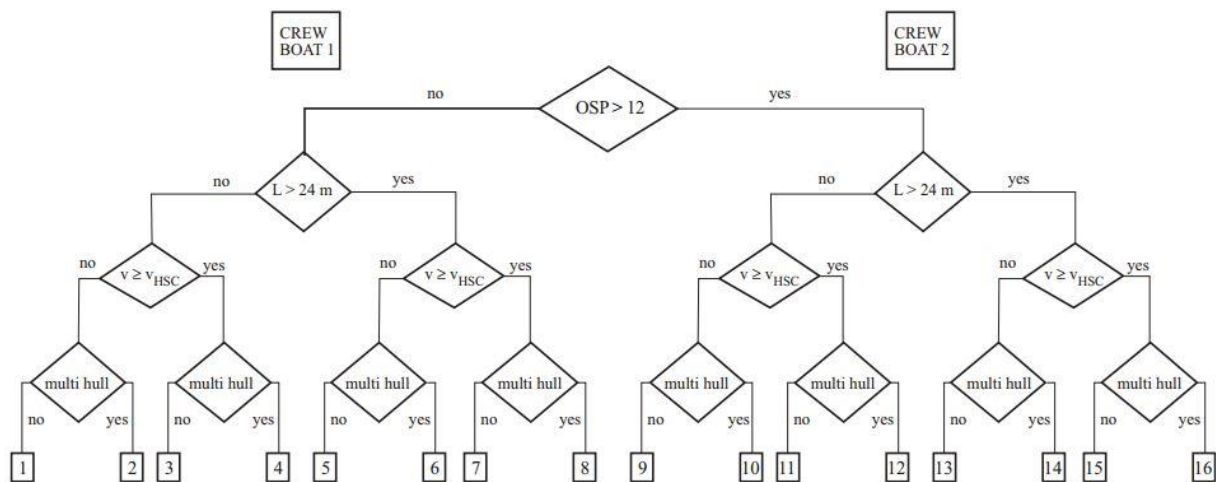


Figure 40 : Scheme for selection of rules to be applied according to the 4 main criteria [9]

In this case, the 25m catamaran is a crew boat of the 8th category and the scantling is designed by following the instructions of the *Rules for classification and construction – 3.1 Special craft/ High Speed Craft* of Germanischer Lloyd [9].

According to Grubisic [6], a first estimation of the structural weight can be established, Table 29.

Table 29 : Estimation of the structural weight of the catamaran [6]

	Formula	Structural weight [t]
Ws	$0.0082 * [L(B+D)]^{1.36}$	21.602

The main elements of the structure for the weight estimation are the hull, the bulkheads, the frames and the decks. A value of the VCG has been obtained from this first weight breakdown. The description of the preliminary structural design is explained in Annex 2.

6.1.5. General arrangement

The catamaran is composed of three decks, the below deck, the main deck and the bridge deck. The machine room, rudder room and bow thruster space are in the below deck level. Three sets of tanks ensure necessary resources to go offshore and come back.

The main deck is on two levels. The aft part until 11 meters from the aft perpendicular is 3.6 meters high from the zero point while the fore part is at 4.6 meters. The deck is raised to provide enough reserve of buoyancy in response of the low underwater volume due to the axe bow configuration. The wheelhouse is located in the aft region of the main deck. The crew living area is on the ground floor of the wheelhouse. It accommodates until 4 persons in two rooms with one bathroom. The day room, store and an additional bathroom are on the starboard part of the wheelhouse, Figure 42.

The first level of the wheelhouse, called bridge deck, is composed of the seats for the passengers, the nautical and communication equipment along with windows at 360° to improve the visibility and comfort of passengers. A cargo deck area of 90m² is at the front of the wheelhouse and a strong bow fender takes the fore part of the catamaran between the two demi-hulls, Figure 41.

Comparison of motion sickness incidence
of three crew transfer vessels with different hull forms

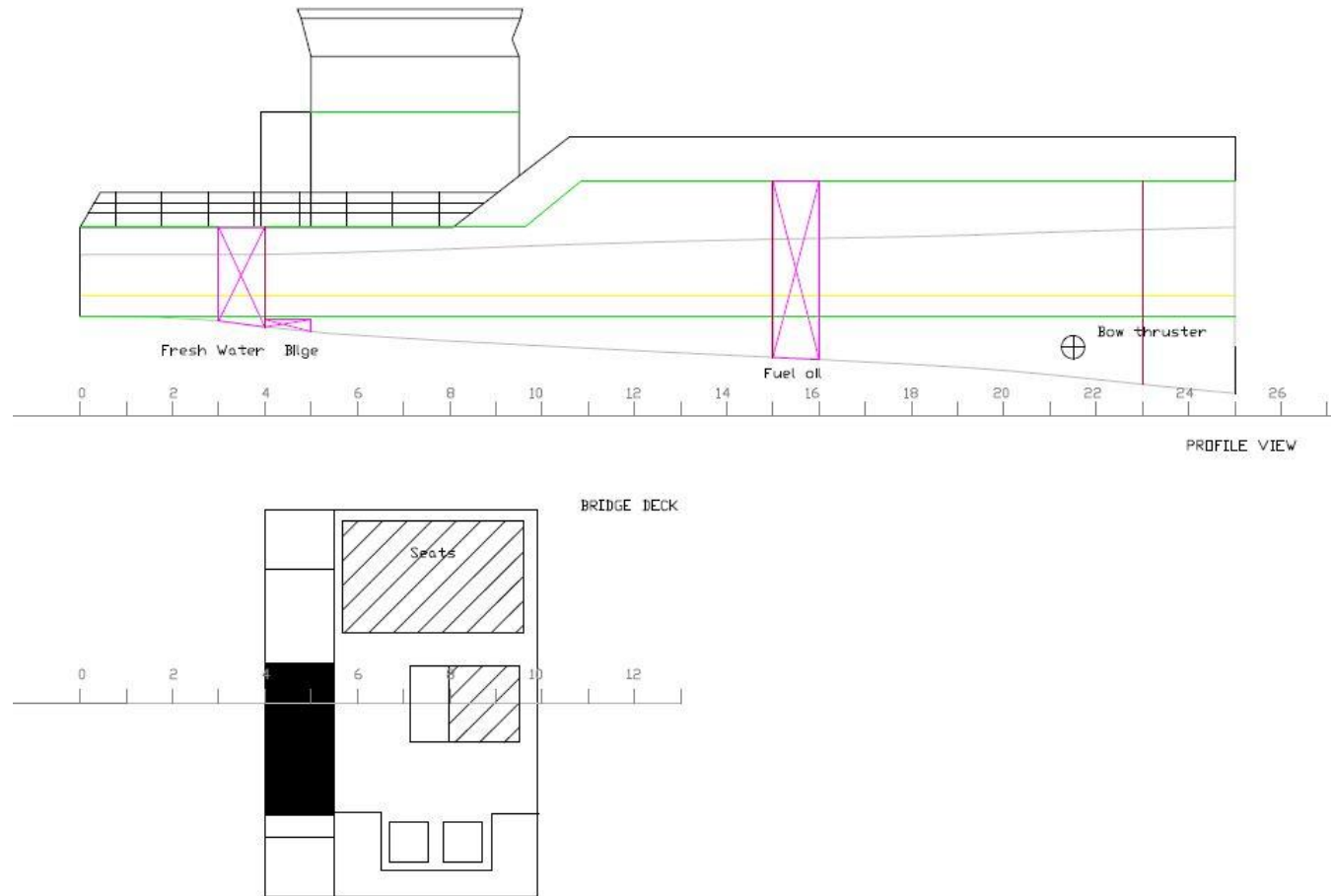


Figure 41 : Profile view and bridge general arrangement of the catamaran

Comparison of motion sickness incidence
of three crew transfer vessels with different hull forms

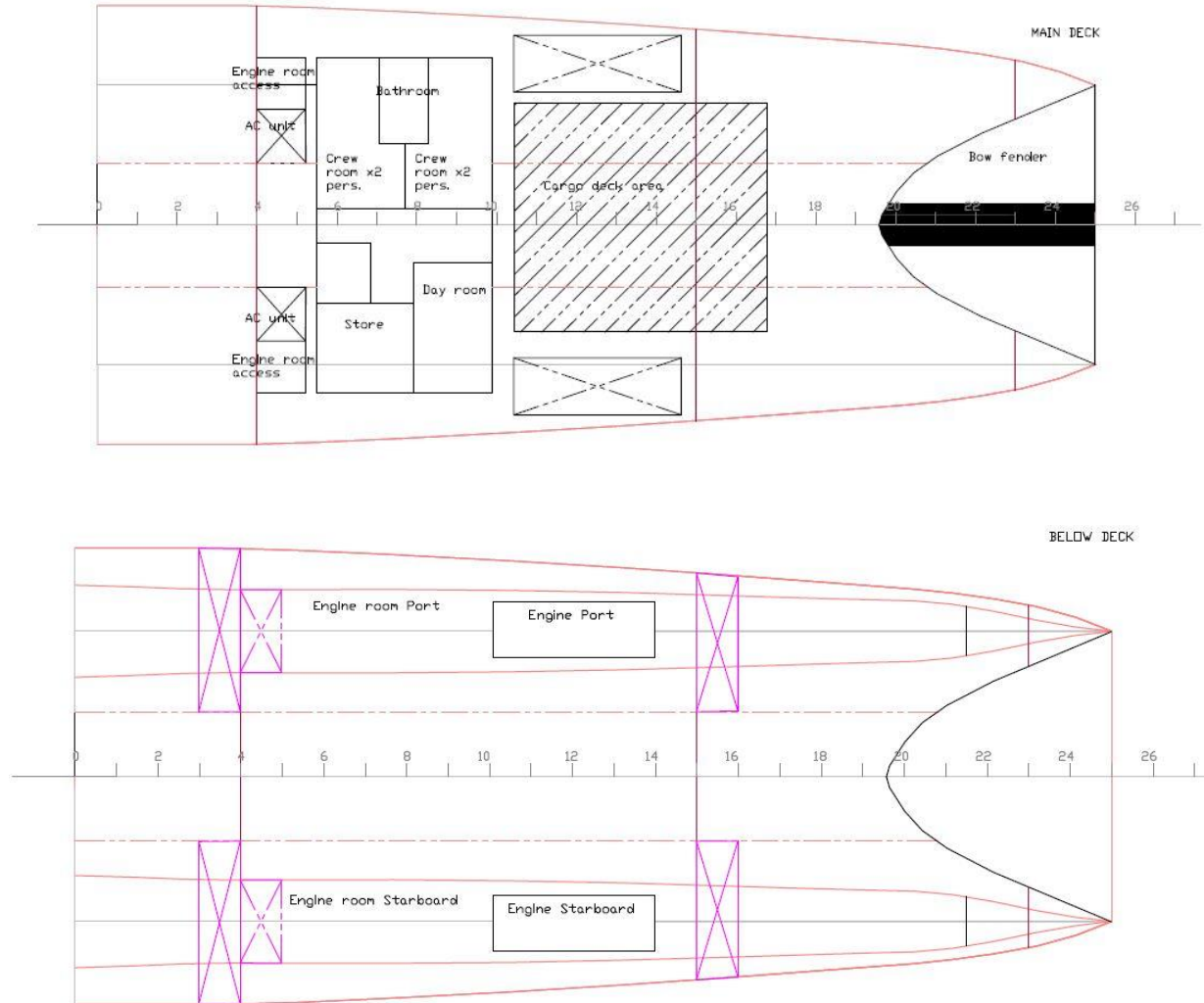


Figure 42 : General arrangement of main and below deck of the catamaran
Master Thesis developed at West Pomeranian University of Technology, Szczecin

6.1.6. Weight estimation of the catamaran

The lightship of the SeaZip is known, 72.8 tonnes. The displacement of the MCS Sirrocco is 80 tonnes with 50% of consumables, ie around 100 tonnes full loaded. The ship carries 14.2m³ of fuel along with 2m³ of water and cargo.

The full loaded displacement was estimated to be equal to 100 tonnes. The main elements of the lightship weight are presented in the Table 30.

Table 30 : Main elements of the lightship weight

	Weight [kg]	LCG[m]	TCG[m]	VCG[m]
Structural weight:				
Structure	17801	7.23	0.00	2.77
Bulkheads & Frames	2300	-0.69	0.00	3.15
Superstructure	1534	7.27	0.00	6.44
Bridge deck	1500	-5.5	0	5
Maindeck:				
Bow fender	350	11.5	0	4.2
Knuckle boom crane	600	8	4	3.6
Anchor + anchor chain	150	23.5	0	3.6
inflated rafts	400	-7.5	0	3.3
Crew living area	2600	-5.5	0	4
Below deck:				
Engines + filling	4200	-1	0	2.7
Propellers + shaft	2000	-9	0	0.5
Gear Boxes	2000	-4	0	2.2
Bow thrusters	1000	9	0	1
Diesel generator	2000	1.5	0	2.7
Rudder + shaft	900	-11	0	1
Steering gear	260	-12	0	2
Lightshipweight	72800	2.578	0.067	3.201

6.1.7. Vertical position of the centre of gravity

The vertical position of the centre of gravity is deduced with the tanks definition, Table 31.

Table 31 : Position of the centre of gravity of the tanks and the « go offshore » load case

	Go offshore load case					
	Quantity (1=100%)	Unit mass [t]	Total mass [t]	Longitudinal arm [m]	Transversal arm [m]	Vertical arm [m]
Lightship	1	72.800	72.800	11.252	0.000	3.080
FuelS	1	7.106	7.106	15.497	3.379	2.723
FuelP	1	7.106	7.106	15.497	-3.379	2.723
FreshWaterS	1	4.868	4.868	3.502	4.160	2.581
FreshWaterP	1	4.868	4.868	3.502	-4.160	2.581
KeelS	1	0.213	0.213	4.532	-3.500	1.494
KeelP	1	0.213	0.213	4.532	3.500	1.494
Total Loadcase			97.174	11.067	0.000	2.971

The vertical position of the centre of gravity of the full loaded load case has been taken equal to 2.971m.

6.2. Numerical model for the catamaran analysis

There is a special way to treat multi-hulls with *Seakeeper*. There is only one demihull which is represented. The demi-hull centreline spacing is defined as in the Figure 43 in *Maxsurf* and then the design with its vessel type configuration is loaded in *Seakeeper*.

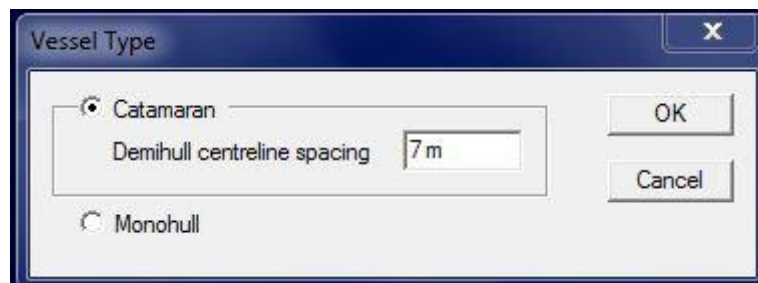


Figure 43 : Vessel type definition according to Maxsurf model

Due to this simplification, the interaction into the two hulls is not taken in consideration during the analysis. The results are more accurate for low speed when the hulls interaction is less representative. Moreover the interaction between hulls is less for head seas. It is not possible to study the impact of demi-hull spacing on the seakeeping behaviour.

The added mass and inertia of roll are calculated from the heave properties of the vessel, moreover the roll damping coefficient is deduced from the heave damping coefficient.

6.3. Results and MSI-curves for the catamaran

Thirteen tests have been done with the catamaran hull configuration, see Table 32. There were four different speeds and significant wave heights along with four wave frequencies.

Table 32 : Simulation conducted with the catamaran

	Speeds [kn]	Hs [m]	Wave frequency [Hz]
C05000	5	2	0.171
C050909			
C05135			
C05180			
C05315			
C10000	10	2	0.146
C10090			
C10135			
C10180			
C10315			
C012180	12	2.4	0.127
C08180	8		0.171
C112180	12	1.5	0.207

The five JONSWAP spectra used to represent the North Sea are presented in the Figure 44.

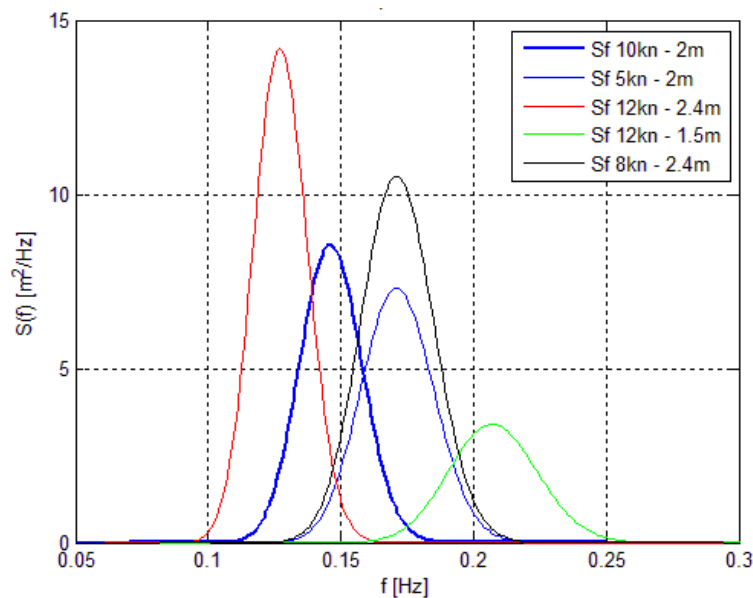


Figure 44 : JONSWAP spectra used for the seakeeping analyses

The maximum significant vertical accelerations and peak period of the encounter spectrum are presented in the Table 33. When the catamaran is navigating at 12 knots in head seas with

2.4m high waves and a period of 7.9sec, the significant vertical acceleration at bow is not realistic. The irrelevant values are not considered to draw the MSI-curves.

Table 33 : Maximal significant vertical acceleration and peak frequencies of the catamaran analyses

Numerical analyses			Physical experiments		
Tests n°	Peak frequency [Hz]	Max. a1/3 [g]	Tests n°	Peak frequency [Hz]	Max. a1/3 [g]
C05090	0.167	0.629	2705090	0.168	0.128
C05135	0.211	0.646	2705135	0.192	0.148
C05180	0.212	0.393	2705180	0.180	0.142
C05315	0.137	0.504	2705315	0.151	0.073
C10090	0.145	0.570	2710090	0.196	0.120
C10135	0.193	0.632	2710135	0.204	0.160
C10180	0.214	0.612	2710180	0.201	0.160
C10315	0.094	0.210	2710315	0.151	0.060
C08180	0.170	0.734	HB08180	0.127	0.167
C012180	0.370	0.790	HB012180	0.207	0.192
C112180	0.193	0.685	HB112180	0.127	0.071

At 5 knots in beam seas, the peak frequency of the ship response spectrum of the catamaran and SWATH are similar but the maximal significant vertical acceleration is 5 times higher for the catamaran. When the SWATH is encountered by beam seas, the main deck stays in a horizontal position

of three crew transfer vessels with different hull forms

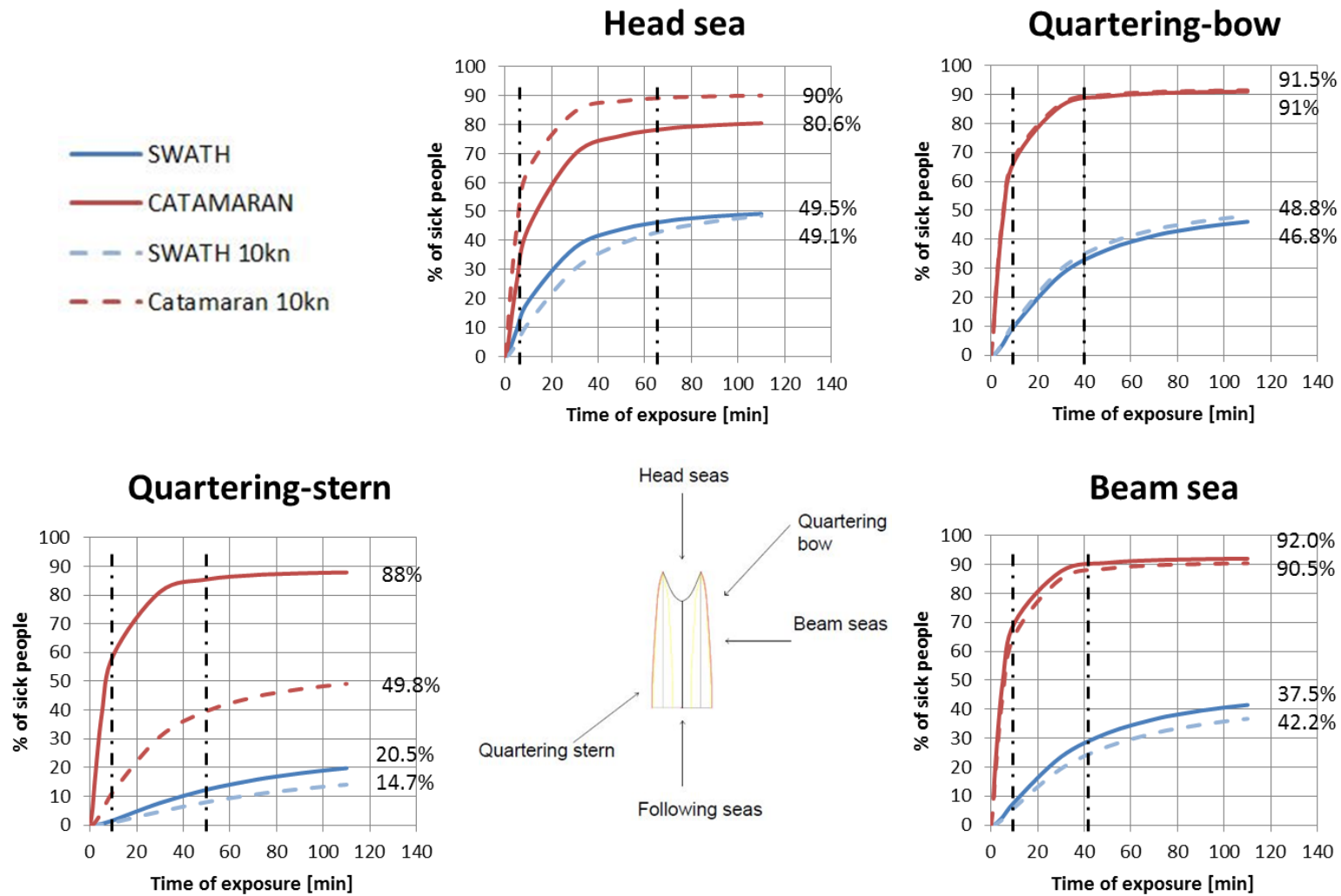


Figure 45 : Results for the 5 and 10 knots simulation of the catamaran

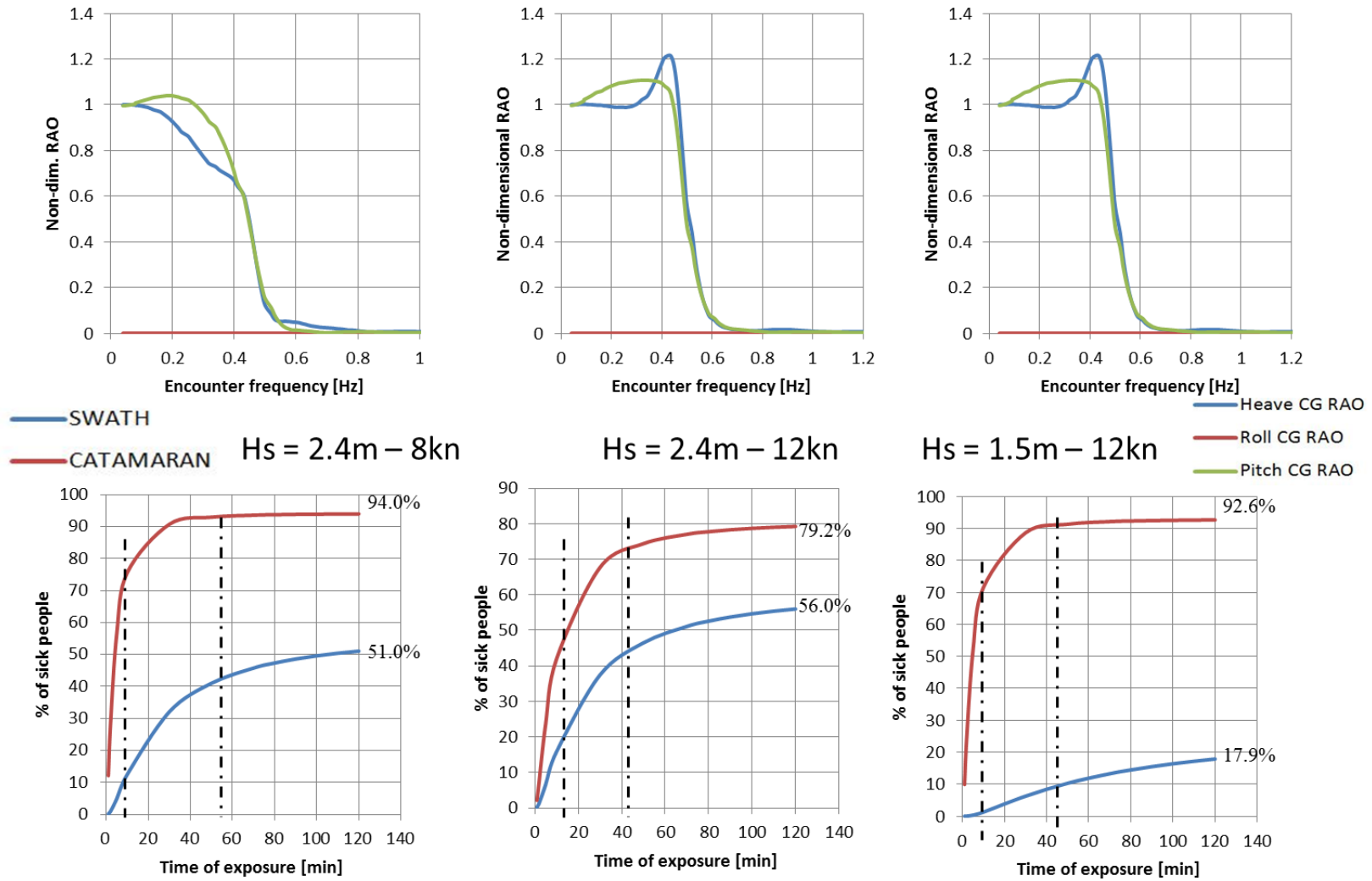


Figure 46 : RAOs of the catamaran and her MSI-curves compared to the SWATH

Comparison at 5 and 10 knots

The trend curves for the catamaran are similar to the monohull, the increasing of motion sickness on board are similar, Table 34. The trend are not representing on the graph to not surcharging them.

Table 34 : Trend curves for the catamaran MSI and SWATH

Tests	Ship	Trend equation	Correlation coefficient R ²
8kn -2.4m	SWATH	$12.25*\ln(x)-7.95$	0.96
	Catamaran	$16.42*\ln(x)+23.0$	0.92
12kn-2.4m	SWATH	$13.41*\ln(x)-7.80$	0.97
	Catamaran	$13.82*\ln(x)+38.27$	0.86
12kn-1.5m	SWATH	$0.259*x-0.69$	0.99
	Catamaran	$16.97*\ln(x)+18.95$	0.93

Table 35 : Difference in term of motion sickness incidence between the Catamaran and the SWATH

Heading angle [°]	Time of exposure [min]	Catamaran vs SWATH	
		5 knots	10 knots
90°	10	8.8	10.8
	50	2.8	3.3
	120	2.2	2.4
135°	10	6.6	6.1
	50	2.5	2.3
	120	1.9	1.9
180°	10	2.3	5.7
	50	1.7	2.3
	120	1.6	1.8
315°	10	35.1	13.4
	50	6.9	4.9
	120	4.3	3.4

The passengers are sicker on catamaran than SWATH, it is depicted in Figure 45 and Figure 46.

The number of sick people on SWATH inches up compared to the catamaran where it soars during the first 20-30 minutes. It is exposed on the Table 35 where the multiplier is higher for 10 minutes.

The 315° heading angle waves are the worst comfortable waves for the catamaran, Table 35. The waves come from the back, it induced decoupled motion between the two demi-hulls of

the ship if the wave length shorter than the ship length. After reaching the stationary state, the passengers are 1.6 to 2.5 times sicker on catamaran for waves from beam to front and 5 times sicker of waves are coming from stern in this configuration.

Instead of having a pitch resonance like the monohull, the catamaran has a resonance frequency in heave motion for head seas. The natural rolling period of a catamaran is generally two times smaller than that of a monohull, the peak resonance in roll will be in shorter waves and then in long waves the catamaran's roll resonance frequency is sufficiently far from the resonance conditions.

The overall slenderness ratio of catamaran hull form is bigger than monohull, then when waves encounter the multihull, the ships will follow the waves instead of cut them. A heave global motion is more pronounced for catamarans than monohulls.

Due to his higher metacentric height, the catamaran has shorter natural rolling period which can cause discomfort. The difference in term of percentage of sick people on board is greater for non-beam seas waves because of this short rolling period.

7. CONCLUSIONS

With the increasing of offshore installations close to the coast, the small crew transfer vessels which are used for daily work are more and more visible in the fleet of north European harbours.

The first steps of preliminary design of ships are driven by comparative designs and naval architect know-how. The main characteristics are initially settled and will be adjusted in the course of the design project, during the tanks definition, structural design or hydrodynamics calculation.

The flexibility in term of decision during the beginning of the project of designing a ship is wide and the modification of one or another parameter/dimension induce an important charge of work and can be expensive. The work can be done many time before getting a satisfied preliminary design such as the monohull and catamaran of this master thesis.

The structural design is a large amount of the first weight breakdown of the ship. There are few scientific papers which treat the case of small boat (less than 50 meters) in comparison with the tanker and bulk-carrier. A scientific paper, written by Grubisic in 2008 was really usefull to get a first approximation of the structural weight of my ships. A more accurate preliminary structural design of the catamaran according to the Germanischer Lloyds rules of classification [9]. Determine the position of the centre of gravity is a heavy task because the first loop of the spiral design has to be completed at 90% to obtain the first estimation (cost estimation not necessary). The vertical position of the centre of gravity is crucial to assess the seakeeping analysis and get the significant vertical accelerations at different location on the bridge.

The motion sickness incidence has been defined by McCaughley and Al. in 1976 [1] with a mathematical formulation to draw the MSI-curve which is function of peak encounter frequency and significant vertical acceleration. This work gives an overview of the seasickness on board. It shows that in average 40-45% of the crew are sicker on monohull and catamaran than SWATH. It is important to keep in mind that the results have taken in consideration the one-third of the highest vertical acceleration. Having two hours of high vertical accelerations like that doesn't happen frequently.

The stabilisation devices where not taken in consideration during the analysis and there play an important role but the time was short to do additional researches concerning the fins which are installed on the monohull and catamaran.

The random ocean waves were modelled according to JONSWAP spectra because the experimental comparative data came from full scale tests in North-Sea. Globally, people are sicker on monohull and catamaran than SWATH even if the speed of the SWATH is smaller for the same amount of power due to her higher resistance.

Additional work could be done to improve the CG calculation and get more accurate results for the simulation. The structural designs and weight estimation can be refined. It could be interesting to get the same displacement for the monohull which is going on-shore and the catamaran. One of next project could be the coupling between a seakeeping computer software and optimisation one such as *Friendship-framework* to get the best hulls for the lower motion sickness incidence after two hours of exposure.

8. ACKNOWLEDGEMENTS

The author wants to thank the company *ABEKING & RASMUSSEN* and in particular Mr. Michael Luehder for his valuable help and continuous supervision.

This master thesis was developed in West Pomeranian University of Technology of Szczecin under the academic supervision of Professor Zbigniew Sekulski and in the frame of the European Master Course in “Integrated Advanced Ship Design” named “EMSHIP” for “European Education in Advanced Ship Design”, Ref. 159652-1-2009-1-BE-ERA MUNDUS-EMMC.

9. REFERENCES

- [1] – “Motion Sickness Incidence: exploratory studies of habituation, pitch and roll, and the refinement of the mathematical model”, Michael E. McCaughley, Jackson W. Royal, C. Dennis Wylie, James F. O’Hanlon, Robert R. Mackie - department of the US navy, April 1976
- [2] – «The effect of bow shape on the seakeeping performance of a fast monohull », Keuning, J.A., Toxopeus, S, Pinkster, Jacob - Fast 2001 conference, September 2001
- [3] - International Code of Safety for High-Speed Craft (HSC Code), IMO (1994 and 2000)
- [4] - White, C., “The cruising multihull”, International Marine, Camden, Maine, 1996]
- [5] - “Human factors for naval marine vehicles design and operation” –
- [5] - Mechanical vibration and shock – Evaluation of human exposure to whole-body vibration” (ISO Standard 2631-1, 1997)
- [6] - Reliability of weight prediction in the small craft concept design, Izvor Grubisic, University of Zagreb – Croatia
- [6] – Report of Duhnen’s experiments (2000)
- [7] – Dubrovsky, V., Lyakhovitsky, A., “Multi-hull ships”
- [8] – Rules for the classification of crew boats, Bureau Veritas classification society - may 2005 (May 2005)
- [9] – Rules for classification and construction ship technology – 6. Offshore Service Vessels – Germanischer Lloyd (2012)
- [10] Sujimoto, R. “Weight estimation of custom motor yachts in the range between 45 and 65 meter length”, EMship master thesis, 2012 (confidential)
- [11] US 8047148 B2 – Abstract of the axe-bow concept patent written by J.A. Keuning, University of Delft, Nov. 2011